Authors:

Taro Kimura[a], Tomoko Tsuchida-Mayama[b], Hirotatsu Imai[a, c], Koji Okajima[d], Kosuke Ito[a], Tatsuya Sakai[a]

[a]Graduate School of Science and Technology, Niigata University, Niigata-shi, Niigata, 950-2181, Japan

[b]RIKEN Plant Science Center, RIKEN Plant Science Center, Yokohama, Kanagawa 230-0045, Japan

[c]Research Fellow of Japan Society for the Promotion of Science, Kojimachi Business Center Building, Chiyoda-ku, Tokyo 102-0083, Japan

[d]Department of Physics, Keio University, 3-14-1, Hiyoshi, Kouhoku-ku, Yokohama, Kanagawa 223-8522, Japan

Corresponding author: Tatsuya Sakai

e-mail: tsakai@gs.niigata-u.ac.jp

Title: Arabidopsis ROOT PHOTOTROPISM2 is a Light-Dependent Dynamic Modulator of Phototropin1

Short title: Action mechanism of RPT2 in phototropism

The author for distribution of materials integral to the findings presented in this article in accordance with the policy described in the Instructions for Authors

23 (www.plantcell.org) is Tatsuya Sakai (tsakai@gs.niigata-u.ac.jp).

24

ABSTRACT

Arabidopsis thaliana phototropin1 (phot1) is a blue-light photoreceptor, i.e. a blue-light-activated Ser/Thr-protein kinase that mediates various light responses including phototropism. Phot1 functions in hypocotyl phototropism dependent on the light induction of ROOT PHOTOTROPISM2 (RPT2) proteins within a broad range of blue light intensities. It is not yet known however how RPT2 contributes to the photosensory adaptation of phot1 to high intensity blue light and the second positive phototropism. We here show that RPT2 suppresses the activity of phot1. Yeast two-hybrid analysis indicated RPT2 binding to the LOV1 (light, oxygen or voltage sensing 1) domain of phot1 required for its high photosensitivity. Our biochemical analyses revealed that RPT2 inhibits the autophosphorylation of phot1, suggesting that it suppresses the photosensitivity and/or kinase activity of phot1 through the inhibition of LOV1 function. We found for the first time that RPT2 proteins are degraded via a ubiquitin-proteasome pathway when phot1 is inactive and stabilized under blue-light conditions in a phot1-dependent manner. We propose that RPT2 is a molecular rheostat that maintains a moderate activation level of phot1 under any light intensity conditions.

INTRODUCTION

Plant life is strongly dependent on light and the angiosperm *Arabidopsis thaliana* uses several kinds of photoreceptors to effectively adapt to various light conditions, including phytochromes (phys) which are red-/far-red-light photoreceptors, cryptochromes (crys), phototropins (phots), the LOV (light, oxygen or voltage sensing)/F-box/Kelch-domain proteins (ZTL, FKF1, and LKP2), which are blue-light photoreceptors, and a UV photoreceptor UVR8 (de Wit et al., 2016). In the case of the phy and cry families, phyA and cry2 are highly expressed in *Arabidopsis* seedlings under dark conditions and become unstable under bright light conditions, thus contributing strongly to the responses to weak and not bright light conditions. (Clough and Vierstra, 1997; Lin et al., 1998; Sharrock and Clack, 2002; Casal et al., 2014). On the other hand, phyB and cry1 are stable and function as major photoreceptors under bright light conditions (Lin et al., 1998; Li et al., 2011). Plants therefore use different photoreceptor families and members of these families to recognize light quality and quantity in order to adapt to their various light environments.

In the case of the phot family, the highly photosensitive photoreceptor phot1 and the less photosensitive photoreceptor phot2 function redundantly in a fluence-rate dependent manner (Sakai et al., 2001). The phots have LOV1 and LOV2 domains in their N-terminal portions, and a serine/threonine (Ser/Thr) kinase domain belonging to the AGC (for cAMP-dependent protein kinase A, cGMP-dependent protein kinase G, and phospholipid-dependent protein kinase

C) VIII kinase domain, within their C-terminal half (Christie, 2007; Rademacher and Offringa., 2012). The phots localize on the inner surface of the plasma membrane, show autophosphorylation activities under blue-light conditions, and mediate blue-light responses such as phototropism, chloroplast photorelocation and stomatal opening (Christie et al., 1998; Kagawa et al., 2001; Kinoshita et al., 2001; Sakai et al., 2001; Sakamoto and Briggs, 2002). Each LOV domain harbors flavin mononucleotide (FMN) as a blue-light absorbing chromophore (Christie et al., 1998; Sakai et al., 2001) and transiently forms a cysteinyl adduct with a blue-light-excited FMN (Christie, 2007). This cysteinyl adduct undergoes thermal decay and LOV domains thus show dark reversion (Okajima, 2016). The photochemical reaction mediated through the LOV2 domain is indispensable for phot function and leads to their conformational change and activation as a Ser/Thr kinase (Christie et al., 2002; Christie, 2007). The lifetime of the cysteinyl-FMN adduct of phot2 LOV2 is 10-fold greater than that of phot1, which appears to be one of reasons why phot2 does not function under low intensity blue light conditions (Okajima et al., 2012). On the other hand, phot1 is a unique photoreceptor that mediates the phototropic responses in etiolated hypocotyls over a broad dynamic range of blue light intensities between 10^{-5} and 10^{2} μmol m^{-2} s^{-1} (Sakai et al., 2001; Haga et al., 2015). The photochemical reaction at the LOV1 of phot1 is unnecessary for the phototropic response (Christie et al., 2002), but this domain itself is necessary for the induction of the phototropic responses under low intensity blue light conditions (Sullivan et al., 2008). The phot1 LOV1

89 domain thus appears to play an important role in the control of phot1
90 photosensitivity, but the precise underlying molecular functions are yet
91 unrevealed.

92 The ROOT PHOTOTROPISM2 (RPT2) protein is a signal transducer in
93 *Arabidopsis* phototropism (Sakai et al., 2000). It localizes on the plasma
94 membrane and forms a complex with phot1 in vivo (Inada et al., 2004). RPT2
95 expression is suppressed in etiolated seedlings and upregulated by red- and/or
96 blue-light irradiation (Sakai et al., 2000; Tsuchida-Mayama et al., 2010). The phys
97 and crys are necessary for the induction of *RPT2* transcription
98 (Tsuchida-Mayama et al., 2010). *Rpt2* loss-of-function mutants exhibit increased
99 responses to very low intensity blue light at 10^{-5} μmol m^{-2} s^{-1} and decreased
100 responses to blue light at 10^{-3} μmol m^{-2} s^{-1} or more during hypocotyl
101 phototropism (Haga et al., 2015). On the other hand, the expression of *RPT2*
102 prior to a phototropic stimulation in etiolated wild-type seedlings accelerates
103 continuous light-induced phototropism (Haga et al., 2015). These findings have
104 suggested that the light induction of RPT2 expression reduces the
105 photosensitivity of phot1, which is required for the photosensory adaptation of
106 phot1 and the second phototropism under bright light conditions (Haga et al.,
107 2015).

108 In our present study, we tested the hypothesis that RPT2 controls the
109 photosensitivity of phot1 through its LOV1 domain. A yeast two-hybrid assay
110 indicated that RPT2 binds to the phot1 LOV1 domain and immunoblotting using

Phos-tag SDS-poly-acrylamide gels indicated that a *rpt2* mutation enhances the autophosphorylation of phot1, and that the *RPT2* overexpression suppresses this. These data indicated that RPT2 controls the autophosphorylation activity of phot1 through the LOV1 domain. We further showed that RPT2 expression is upregulated not only by the phys and crys but also by phots. Based on our current results, we propose that RPT2 acts as a molecular rheostat that maintains a moderate activation of phot1 under any light intensity conditions.

RESULTS

RPT2 binds to the LOV1 domains of phot1

Our previous study demonstrated that the N-terminal half of RPT2 (RPT2 N) including the BTB/POZ (broad complex, tramtrack and bric-à-brac/Pox virus and zinc finger) protein-protein interaction domain binds to the N-terminal half of PHOT1 that includes two LOV domains (Inada et al*.,* 2004). We divided the N-terminal half of PHOT1 into 4 fragments and examined RPT2 N binding to these fragments or its kinase domain (PHOT1 C) using a yeast two-hybrid assay (Figure 1A: Inada et al., 2004). As shown in Figure 1B, RPT2 N bound only to the LOV1 domain (PHOT1 N2). We confirmed its binding using an in vitro pull-down assay. The hemagglutinin-tagged (HA-) RPT2 N proteins specifically interacted with the histidine/ProS2-tagged (His-) PHOT1 N2 proteins on metal affinity resins in contrast with His-PHOT1 N4 harboring the LOV2 domain (Figure 1C). These results suggest that RPT2 affects phot1 photosensitivity via the LOV1 domain.

Christie et al. (2002) reported previously that by using the LOV1Cys39Ala mutant, the LOV1 domain of phot1 is photochemically active but that its photochemical reaction is unessential for phot1 function. Our current yeast two hybrid assay data showed that the LOV1 domain harboring a Cys39Ala mutation (PHOT1 N2mut) also binds to RPT2 N as well as PHOT1 N2 (Figure 1B). Furthermore, the *phot1 phot2* transgenic seedlings expressing the *PHOT1* gene with the LOV1Cys39Ala mutation showed a shortened time lag to the induction of phototropic responses by a red-light pretreatment (Supplemental Figure 1), which is dependent on *RPT2* (Haga et al., 2015). Our previous study had already indicated that RPT2 can form a complex with phot1 in vivo under both conditions of darkness and blue light (Inada et al., 2004). These results suggest that RPT2 binding and function are unaffected by the photochemical reaction of the phot1 LOV1 domain and the phosphorylation state of phot1.

RPT2 suppresses the autophosphorylation of phot1

Our previous genetic study suggested that RPT2 reduces the photosensitivity of phot1, which is required for a second positive phototropism under bright light conditions (Haga et al., 2015). This indicated that RPT2 may suppress the activity of phot1. To test this possibility, we examined the autophosphorylation pattern of phot1 in both wild-type *Arabidopsis* seedlings and *rpt2* mutants grown on the surface of vertically oriented agar medium. We conducted immunoblotting analysis using a Phos-tag acrylamide gel for this experiment (Kinoshita and

Kinoshita-Kikuta, 2011), in which the migration of phosphorylated proteins is specifically retarded. We observed autophosphorylation patterns of phot1 in response to blue-light irradiation for 2 h at 0.001, 0.1 and 100 μmol m^{-2} s^{-1} (Figure 2A). When the wild-type seedlings were irradiated, the mobilities of PHOT1 proteins became much slower if the fluence rates were higher (Figure 2A). These mobility shifts were more clearly observed using a Phos-tag acrylamide gel (+Phos-tag) compared with a normal SDS-polyacrylamide gel (–Phos-tag: Figure 2A). This result suggested that the autophosphorylation activity of phot1 increases as the fluence rates increase.

We next investigated the autophosphorylation pattern of phot1 during blue light irradiation. When we monitored the phosphorylation status of the PHOT1 protein under blue light conditions at 100 μmol m^{-2} s^{-1} (Figure 2B), mobility shifts of this protein were detectable at 1 hour, but further irradiation suppressed phot1 autophosphorylation in parallel with the accumulation of RPT2 proteins. Under blue light conditions at 0.1 μmol m^{-2} s^{-1}, mobility shifts in the PHOT1 proteins were marginally detectable at 1 min, became saturated at 30 min, but were suppressed at 60 and 120 min after the onset of irradiation in wild-type etiolated seedlings (Figure 2C).

Arabidopsis wild-type hypocotyls show a delayed phototropic response when grown along the surface of vertically oriented agar medium and a quick response when grown on the agar medium without touching the agar medium (Haga and Sakai, 2012; Sullivan et al., 2019). We examined the

177 autophosphorylation of phot1 in wild-type *Arabidopsis* seedlings grown on agar
178 medium in 0.2 ml tubes (Haga et al., 2012). They showed similar phot1
179 autophosphorylation patterns to those in the seedlings grown on vertically
180 oriented agar medium (Supplemental Figure 2), suggesting that the phot1
181 autophosphorylation activity in seedlings is unaffected by the friction or the
182 moisture between the agar surface and the shoots. We therefore used the
183 seedlings grown on the surface of vertically oriented agar medium in later
184 analyses.

185 In the –Phos-tag gel, the *rpt2* mutation did not produce any obvious
186 effect on the mobility shifts of the PHOT1 proteins (Figure 2A), as reported
187 previously (Inada et al., 2004; Haga et al., 2015). However, in the +Phos-tag gel,
188 the *rpt2* mutation appeared to cause a pronounced mobility shift in the PHOT1
189 protein under blue light conditions at 0.001, 0.1 and 100 μmol m^{-2} s^{-1} (Figure 2A).
190 The mobility shift of PHOT1 with the *rpt2* mutation disappeared when the
191 extracted proteins were treated with alkaline phosphatase (Supplemental Figure
192 3), indicating that its shift reflects differences in phosphorylation state of PHOT1.
193 Interestingly, the *rprt2* mutants did not exhibit any attenuation of phot1
194 autophosphorylation at 2, 4 and 6 hours (Figure 2B) or at 60 and 120 min (Figure
195 2C) after the onset of blue-light irradiation of 100 and 0.1 μmol m^{-2} s^{-1},
196 respectively. On the other hand, a constitutive *RPT2* expression line
197 (*35Spro:RPT2*: Haga et al., 2015) showed an attenuation of
198 phot1-autophosphorylation at 30 min after the onset of the blue-light irradiation

(Figure 2C). These results suggested that RPT2 proteins can suppress the autophosphorylation or enhance the dephosphorylation of phot1 and that a loss-of-function mutation in *RPT2* leads to a continuous hyperactivation of phot1 in seedlings.

The effect of RPT2 on the autophosphorylation of phot2 was also examined using an anti-PHOT2 antibody, which recognizes both PHOT1 (~120 kDa) and PHOT2 (~110 kDa: Supplemental Figure 4). When wild-type seedlings were irradiated with blue light at 0.001, 0.1, and 100 μmol m^{-2} s^{-1}, mobility shifts in the PHOT2 proteins were detectable only at 100 μmol m^{-2} s^{-1} (Figure 2D, dotted area). Under blue-light conditions of 100 μmol m^{-2} s^{-1}, the mobility shifts of the PHOT2 proteins were marginally detectable at 1 min, saturated at 30 min, and attenuated at 120 min after the onset of the irradiation in wild-type etiolated seedlings (Figure 2E). Those autophosphorylation patterns were also detected in the *rpt2* mutants and the *35Spro:RPT2* transgenic lines (Figure 2E and 2F). Although green fluorescent protein (GFP)-fused phot2 formed a complex with RPT2 in vivo (Supplemental Figure 5A and 5B) and RPT2 N showed binding activity to the phot2 LOV1 domain in yeast (Supplemental Figure 5C), the results of our phenotypic analysis suggested that RPT2 has no significant impact on the autophosphorylation of phot2. This finding was consistent with the finding of a previous study that the *rpt2* mutation has no effect on phot2-dependent phototropic responses (Inada et al., 2004).

We next examined the inhibitory effects of RPT2 on the

221 autophosphorylation activity of phot1 using an in vitro phosphorylation assay
222 (Figure 3). This assay was performed with microsomal proteins extracted from
223 *rpt2* mutants transformed with a *pMDC7-RPT2* construct, in which the expression
224 of RPT2 is inducible by estradiol (Est) treatment (Supplemental Figure 6: Zuo et
225 al., 2000). The autophosphorylation of phot1 was detected as a radiolabeled 120
226 kDa protein in the microsomal fraction as described previously (Liscum and
227 Briggs, 1995). As expected, blue-light irradiation caused the phosphorylation of
228 these 120 kDa proteins in the microsomal fractions of the *pMDC7-RPT2*
229 seedlings and *pER8* vector control line (Figure 3A). On the other hand, Est
230 treatments suppressed this phot1 phosphorylation in the *pMDC7-RPT2*
231 seedlings but not in the *pER8* vector control line (Figure 3). Our immunoblotting
232 analysis confirmed that PHOT1 protein expression was comparable among all of
233 the microsomal fractions and that the RPT2 proteins were expressed only in the
234 microsomal fraction of Est-treated *pMDC7-RPT2* seedlings (Supplemental
235 Figure 6B). These results suggested that Est-induced RPT2 proteins suppress
236 the in vitro autophosphorylation of phot1.

237 Our present analyses suggested that RPT2 proteins either suppress
238 phot1 autophosphorylation or enhance its dephosphorylation. If a loss-of-function
239 mutation in *RPT2* leads to an enhanced phosphorylation of phot1 due to a block
240 in its dephosphorylation and RPT2 overexpression enhances its
241 dephosphorylation, treatments with protein phosphatase inhibitors seemed to
242 impair the effects of a loss-of-function mutation and overexpression of *RPT2*. We

243 therefore next examined the effects of protein phosphatase inhibitors in the *rpt2*
244 mutants and the *35Spro:RPT2* transgenic lines by immunoblotting analysis using
245 a Phos-tag acrylamide gel. First, we examined the effects of the protein
246 phosphatase inhibitors cantharidin (CN) or okadaic acid (OKA) on the
247 dephosphorylation of phot1. Autophosphorylated PHOT1 proteins in the
248 wild-type seedlings with a pulse irradiation of blue light for 2 min at 100 μmol m^{-2}
249 s^{-1} were dephosphorylated with a subsequent dark incubation for 14 min
250 (Supplemental Figure 7). When the seedlings were treated with CN or OKA, the
251 mobility of the PHOT1 protein became slightly retarded in Phos-tag SDS-PAGE
252 (Supplemental Figure 7). These results indicated that CN and OKA have some
253 inhibitory effects on phot1 dephosphorylation.

254 We next examined the effects of these inhibitors in the *rpt2* mutants.
255 When wild-type seedlings were irradiated with blue light for 0.5 h in the CN- or
256 OKA-containing medium with a red-light pretreatment (for the induction of RPT2:
257 Haga et al. 2015), the PHOT1 proteins showed a hyper mobility shift in contrast to
258 the untreated seedlings (Figure 4A). The phosphorylation of phot1 was enhanced
259 in the *rpt2* mutants in comparison with those in wild-type seedlings independently
260 of the treatments of CN or OKA (Figure 4A). The effects of CN and OKA in the
261 *35Spro:RPT2* transgenic line were also examined (Figure 4B). Red light
262 pretreatment was not done here to ensure that RPT2 expression was not induced
263 in the wild-type seedlings. Constitutive expression of RPT2 suppressed the
264 phosphorylation of phot1 in the *35Spro:RPT2* transgenic lines without being

affected by the CN and OKA treatments (Figure 4B). These results suggested that RPT2 suppresses the autophosphorylation activity of phot1 but does not enhance the dephosphorylation of phot1.

RPT2 is induced by blue-light irradiation in a post-transcriptional manner

Our current results suggested that the induction of RPT2 expression by light irradiation is an important mechanism for controlling both photosensitivity and the autophosphorylation activity of phot1. We thus investigated the light inducibility of RPT2 expression in more detail. We first observed the RPT2 expression patterns using transgenic plants carrying the *RPT2pro:GUS* gene and the *RPT2pro:RPT2-VENUS* gene. GUS staining was detected in a root tip under darkness in the 2-day-old etiolated seedlings carrying the *RPT2pro:GUS* gene (Figure 5A, 5D, and 5G). Both red- and blue-light irradiation enhanced its expression in whole seedlings, most notably the hypocotyls, hooks, and root tips including the elongation zone, in a similar manner (Figure 5B, 5C, 5E, 5F, 5H, and 5I). When the expression patterns of the *RPT2pro:RPT2-VENUS* gene in the *rpt2* mutants were analyzed, we noticed a clear induction of RPT2-VENUS proteins in the aerial part of seedlings (Figure 5L and 5S), especially the elongation zones of the hypocotyls (Figure 5O), and the elongation zone of roots (Figure 5R), but only under blue-light irradiation and not red-light irradiation (Figure 5K, 5N and 5Q). These results indicated that both red- and blue-light irradiation can activate the *RPT2* promoter but that only blue-light irradiation can

induce the RPT2-VENUS proteins effectively.

The accumulation of RPT2 proteins is enhanced by phot activation

The RPT2-VENUS fluorescent signal was detectable in the elongation zones of hypocotyls and roots (Figure 5O and 5R), in which the strong expression of phot1 have been reported (Sakamoto and Briggs, 2002). Thus, we hypothesized that RPT2 proteins are unstable under red-light conditions and that phot1 stabilizes them under blue-light conditions. We tested this using immunoblotting analysis. When the wild-type seedlings were irradiated for 6 hours with red or blue light at 10 μmol m^{-2} s^{-1}, RPT2 protein expression was induced in both cases but blue-light irradiation was much more effective (Figure 6A and 6B). On the other hand, the accumulation of RPT2 proteins under blue-light conditions was attenuated in the *phot1* mutants, which was statistically significant (Figure 6A and 6B). The mutation of the *NPH3* gene, which is required for the phot1 signaling during phototropism (Motchoulski and Liscum, 1999), also caused a decrease of RPT2 accumulation under blue-light conditions (Figure 6A and 6B). Neither *phot1* nor *nph3* mutations affected the red-light induced accumulation of RPT2 (Figure 6A and 6B). qRT-PCR analysis confirmed that the blue-light induction of *RPT2* transcripts was not affected by mutations of *phot1* and *nph3* (Figure 6C). These results suggested that phot1 and its associated protein NPH3 contribute to the accumulation of RPT2 proteins under blue-light conditions in a post-transcriptional manner.

We next examined whether the sole activation of the phot1 photoreceptor is sufficient for the accumulation of RPT2 proteins using *phot1* mutants transformed with a *pMDC7-PHOT1*^{I608E} construct, in which constitutively active PHOT1 proteins (PHOT1^{I608E}: Harper et al., 2004) are inducible by Est treatment. In the etiolated seedlings of the *pER8* vector control line, Est treatment had no effect on the RPT2 protein levels or the phosphorylation status of the NPH3 protein (Figure 6D). On the other hand, in the *phot1* mutants transformed with a *pMDC7-PHOT1*^{I608E} construct (#1 and #2), Est exposure caused the accumulation of RPT2 protein in the absence of blue-light irradiation. This suggested that the accumulation of RPT2 can be caused by phot1 activation alone, even in darkness.

The mobility shift of the NPH3 protein, which reflects a phot1-induced dephosphorylation (Pedmale and Liscum, 2007; Tsuchida-Mayama et al., 2008), was also observed in the #2 transgenic line (Figure 6D), suggesting that *phot1*^{I608E} expression can cause NPH3 dephosphorylation under darkness. A previous study reported that the expression of *PHOT1*^{R472H}, which is another constitutively active variant of phot1, was not sufficient to promote NPH3 dephosphorylation under darkness (Petersen et al., 2017). The discrepancies between the prior result and our current observations may be due to differences in the natures of phot1^{I608E} and phot1^{R472H} and/or the transgene expression levels.

We next analyzed the fluence-rate and time dependence of RPT2

protein accumulation. When wild-type seedlings were irradiated with blue light at 0.01 to 100 μmol m^{-2} s^{-1} for 6 hours, the RPT2 protein levels were increased as the fluence rates of blue light increased (Figure 6E). This induction seemed to be caused by both a transcriptional regulation of phy and cry (Tsuchida-Mayama et al., 2010) and a post-transcriptional regulation of phot1. In the *phot1* mutants, a weakened induction of the RPT2 protein was observed at all fluence rates examined (Figure 6E), suggesting that phot1 contributes to RPT2 accumulation, at least between 0.01 to 100 μmol m^{-2} s^{-1}. In the *phot1 phot2* double mutants, the blue-light induction of RPT2 at 100 μmol m^{-2} s^{-1} was obviously lower than that in the *phot1* single mutant (Figure 6E), suggesting that phot2 also contributes to the accumulation of RPT2 proteins at 100 μmol m^{-2} s^{-1}. When the seedlings were irradiated by blue light at 0.1 or 10 μmol m^{-2} s^{-1} for various times, the induction of RPT2 proteins was detectable at least after 1 hour of the onset of irradiation in both wild type and *phot1* seedlings, but at a higher level in wild type (Figure 6F and 6G). This observation suggested that both the transcriptional induction of *RPT2* by phys and crys (Tsuchida-Mayama et al., 2010) and the post-transcriptional induction of phot1 contributes to an early induction of RPT2 under both fluence-rate conditions.

Previous study has indicated that phot1 is localized to the plasma membrane region in the epidermal cells and the cortical cells of both root and hypocotyl of Arabidopsis etiolated seedlings (Sakamoto and Briggs, 2002). When the *rpt2* transgenic seedlings expressing RPT2-VENUS were irradiated by blue

353 light from above, a fluorescent image of a transverse section of upper hypocotyls
354 showed that the RPT2-VENUS proteins were localized to the plasma membrane
355 region in all tissues of hypocotyls and were strongly expressed in the cortex
356 (Figure 7A). These expression and subcellular localization patterns were similar
357 with those of phot1 (Sakamoto and Briggs, 2002).

358 Suzuki et al. (2019) has reported that unilateral irradiation of blue light
359 induces the asymmetric distribution of phosphorylated Zmphot1 in coleoptiles of
360 *Zea mays* in response to the gradient of blue light intensity in these organs. When
361 the seedlings were unilaterally irradiated, the RPT2-VENUS proteins were often
362 expressed more strongly on the irradiated side of the hypocotyls than on the
363 shaded side (~55% of seedlings; Figure 7B and 7C). On the other hand, there
364 were also seedlings showing symmetric expression patterns (~21%) or a strong
365 expression of RPT2-VENUS on the shaded side (~24%). As the light induction of
366 endogenous RPT2 proteins was already detectable at 1 h after the onset of blue
367 light irradiation at 10 μmol m^{-2} s^{-1} in the immunoblotting analysis (Figure 6E),
368 their distribution patterns at 1 h could also be observed. The RPT2-VENUS
369 fluorescent signal, however, was barely detectable (data not shown). One hour of
370 irradiation seemed to be too short for the expression, maturation and
371 accumulation of RPT2-VENUS proteins to detect its fluorescence. Therefore, we
372 could not draw any conclusions regarding the asymmetric induction of RPT2 in
373 hypocotyls irradiated by unilateral blue light in our present study.
374

RPT2 proteins are degraded through the ubiquitin-proteasome pathway

We examined whether the RPT2 protein is degraded through a ubiquitin-proteasome pathway. When etiolated seedlings of wild type and *phot1 phot2* double mutants were treated with the proteasome inhibitor MG132 for 3 hours under blue light conditions at 10 μmol m^{-2} s^{-1}, RPT2 protein accumulated in the double mutant but not in wild type. This suggested that the *phot1 phot2* double mutants showed a destabilization of RPT2 proteins in a proteasome-dependent manner (Figure 8A). In addition, exposure to MG132 led to the accumulation of RPT2 in wild-type seedlings under red-light conditions but not under blue-light conditions (Supplemental Figure 8). These results suggested that RPT2 is degraded in a proteasome-dependent manner and is stabilized though the activation of phototropins.

To detect polyubiquitinated RPT2 under red-light irradiation, we attempted to immunoprecipitate it from extracts of *UBIQUITIN3* (*UBQ3*) overexpression lines (*35Spro:UBQ3*). Although this was not successful, we unexpectedly found a significant decrease of RPT2 protein in the *35Spro:UBQ3* transgenic lines under both red- and blue-light conditions (Figure 8B). Correspondingly, these transgenic lines showed an abnormality in hypocotyl phototropism i.e. their phototropic curvatures were moderate under weak intensity blue-light conditions and decreased as the fluence rate increased (Figure 8C), in a comparable manner to the *rpt2* mutants (Haga et al., 2015). On the other hand, *UBQ3* overexpression had no effect on the expression patterns of

PHOT1, PHOT2 or NPH3 (Figure 8B), or on the growth of seedlings (Supplemental Figure 9A and 9B). These results suggested that the RPT2 proteins are degraded through the ubiquitin-proteasome pathway and that the activation of phot1 and phot2 may negatively regulate the polyubiquitination of RPT2 proteins and/or its degradation by proteasomes.

DISCUSSION

Our current results demonstrate that RPT2 suppresses the autophosphorylation of phot1 under blue-light conditions. Previous studies have indicated that the phot1 LOV1 domain is necessary for the induction of the phototropic responses under low intensity blue-light conditions (Sullivan et al., 2008) and that the light induction of RPT2 expression suppresses phot1 photosensitivity, which is required for the photosensory adaptation of phot1 to high intensity blue light (Haga et al., 2015). These prior results and our current data suggest that RPT2 negatively regulates the autophosphorylation of phot1 through the LOV1 domain, which is probably required for a formation of a suitable gradient of phot1 activity between the irradiated side and the shaded side in accordance with the high intensity unilateral blue light. Hence, this is the photosensory adaptation mechanism of phot1 in the second positive phototropism of Arabidopsis etiolated hypocotyls. The expression level of RPT2 proteins is increased in response to an increase of blue light intensity (Figure 6E), indicating that RPT2 functions as a molecular rheostat that maintains a moderate activation level of phot1 in etiolated

419 hypocotyls of *Arabidopsis* seedlings under any light intensity conditions.

420 The molecular mechanisms by which RPT2 functions in the suppression
421 of phot1 activity remain to be elucidated. Some prior studies have suggested that
422 the LOV1 domain mediates the dimerization of phot1, which thereby enhances
423 the autophosphorylation of this blue-light photoreceptor (Nakasako et al., 2004;
424 Xue et al., 2018). Thus, RPT2 may inhibit the LOV1-mediated dimerization of
425 phot1 to suppress its kinase activity. Previous studies had also suggested that
426 LOV1 suppresses the decay of the cysteinyl-FMN adduct of LOV2 and enhances
427 the Ser/Thr kinase activity of the phots (Kaiserli et al., 2009; Okajima et al., 2012;
428 Okajima 2016). RPT2 may enhance the decay of the cysteinyl-FMN adduct of
429 phot1 LOV2 through the binding to LOV1 and thus suppress the Ser/Thr kinase
430 activity of phot1. Although our current results suggest that RPT2 suppresses the
431 autophosphorylation activity of phot1, the possibility of enhancement of phot1
432 dephosphorylation by RPT2 still cannot be excluded. RPT2 might play a role as a
433 scaffold of protein phosphatases to dephosphorylate phot1. We also need to
434 examine in the future whether a defect of RPT2 binding to the LOV1 domain
435 indeed affects the autophosphorylation of phot1. Further studies are warranted to
436 elucidate the mechanisms underlying the function of the LOV1 domain and RPT2
437 in phototropin photoactivation in more detail.

438 The post-transcriptional regulation of RPT2 forms a negative feedback
439 loop of phot1 activation. This regulation appears to ensure the formation of a
440 gradient of phot1 signaling activity between the irradiated and shaded sides of

441 plant organs under a broad range of blue-light intensity. This gradient then seems
442 to induce light-induced differential growth including not only phototropic
443 responses but also leaf flattening and cotyledon/leaf positioning (Sakai et al.,
444 2000; Harada et al., 2013). Previous studies have reported that unilateral blue
445 light irradiation results in differential NPH3 aggregate formation in response to
446 phot1 activity across the etiolated hypocotyl, which suppresses and fine-tunes
447 NPH3 activity (Sullivan et al., 2019), and that the light-induced RPT2 proteins
448 suppresses the dephosphorylation and aggregation of NPH3 proteins in the
449 etiolated seedlings (Haga et al., 2015). Our current study findings strongly
450 suggest that RPT2 indirectly suppresses their dephosphorylation and
451 aggregation through the suppression of phot1 activity. On the other hand, our
452 current study results also indicate that NPH3 partially contributes to the
453 stabilization of RPT2 proteins under blue-light conditions (Figure 6B). Thus, the
454 aggregation of NPH3 proteins might decrease the stabilization of RPT2 proteins
455 at the irradiated side and fine-tune the phot1 activity at both the irradiated and the
456 shaded side. Both adjustments of the light induction of PRT2 and of the plasma
457 membrane localization of NPH3 probably contribute to the fine-tuning of phot1
458 signaling across hypocotyls, and an induction of phototropic responses under
459 various light conditions in the etiolated seedlings of *Arabidopsis*. On the other
460 hand, RPT2 is not required for the second positive phototropism in de-etiolated
461 hypocotyls of Arabidopsis seedlings (Sullivan et al., 2019). Other unknown
462 factors and/or mechanisms may suppress the excessive activation of phot1 in

463 green seedlings.

464 Our current observations indicate that RPT2 is degraded by the
465 ubiquitin-proteasome pathway and that phot1 activation suppresses this
466 degradation. This is the first demonstration of a protein stabilization control
467 function of the phots. The mechanism by which the RPT2 protein is ubiquitinated
468 or stabilized under blue-light conditions has been a question of some importance.
469 NPH3 is an essential signal transducer during phototropism and shows binding
470 activity towards RPT2 and possesses ubiquitin E3 ligase activity with Cullin3
471 (Motchoulski and Liscum, 1999; Inada et al., 2004; Roberts et al., 2011). Although
472 we speculated that NPH3 may ubiquitinate RPT2 and promote its degradation
473 under red-light conditions, our immunoblotting analysis revealed that NPH3
474 contributes to its accumulation under blue-light conditions (Figure 6A). As RPT2
475 belongs to the same protein family as NPH3 and also has a BTB/POZ domain
476 which often interacts with Cullin3 (Genschik et al., 2013), it may be ubiquitinated
477 on its own, and its binding to the active forms of the phots may suppress its
478 polyubiquitination and degradation. The issue of whether phot1 controls a
479 ubiquitin-proteasome pathway also remains to be resolved.

480 *RPT2* belongs to the *NPH3/RPT2-like* (*NRL*) gene family (Sakai, 2005)
481 and other NRL members might also have a similar function to RPT2. RPT2 did
482 not show an obvious effect on the suppression of the phot2 activity, although it
483 can bind to its LOV1 domain and form a complex with phot2 in vivo. However, for
484 example, NRL PROTEIN FOR CHLOROPLASTMOVEMENT1 (NCH1) functions

485 in the chloroplast accumulation response in parallel with RPT2 (Suetsugu et al.,
486 2016). Suetsugu et al. (2016) revealed that *nch1* mutants show an enhancement
487 of the phot2-induced avoidance response. One of the hypotheses from this is that
488 NCH1 suppresses the photosensitivity and/or photoactivation of phot2 with
489 RPT2. Thus, the relationships between the NRL members and phototropins in
490 various plants should be reexamined in future studies.
491
492 **METHODS**
493
494 **Plant Materials and Growth Conditions**
495 *Arabidopsis thaliana* ecotype Columbia (Col) was used as the wild type control.
496 Mutant seeds of *rpt2-2* (Col background) and *nph3-102* (Salk_110039; Col
497 background) were obtained as described previously (Inada et al., 2004;
498 Tsuchida-Mayama et al., 2008). The *phot1*-Salk146058 (Col background) and
499 *phot2*-Salk142275 mutants (Col background) were obtained from the
500 Arabidopsis Biological Resource Center (Alonso et al., 2003) and crossed to
501 obtain a *phot1 phot2* double mutant. The *rpt2-2* mutants transformed with a
502 *35Spro:RPT2* gene or a *RPT2pro:RPT2-VENUS* gene were prepared as
503 described previously (Tsuchida-Mayama et al., 2010; Haga et al., 2015).
504 Transgenic Col lines harboring a *RPT2pro:GUS* gene were also prepared as
505 described previously (Inada et al., 2004). The *phot1 phot2* mutants transformed
506 with a *35Spro:PHOT1*^{LOV1Cys39Ala} gene were kindly provided by Professor John

Christie (University of Glasgow).

The *pMDC7-RPT2* transgenic lines were generated as follows. The *RPT2* coding region was subcloned into the entry vector pENTR/D-TOPO (Invitrogen) and shuttled via an LR clonase reaction (Invitrogen) into the estrogen (Est)-inducible vector pMDC7 (Curtis and Grossniklaus, 2003), which was kindly provided by Professor Nam-Hai Chua (Rockefeller University, New York, NY). The *pMDC7-RPT2* plasmid was used for the transformation of *Agrobacterium tumefaciens*, which was then used for subsequent transformations of *rpt2-2* mutants. Several independent *rpt2* transgenic lines showed phototropism complementation following Est treatment (Supplemental Figure 6A). pER8 is an original vector of pMDC7 that lacks the Gateway cassette (Zuo et al., 2000) and was used for the transformation of *A. tumefaciens*, which was then used for subsequent transformations of Col wild type for use as a vector control line.

The *pMDC7-PHOT1*^{I608E} transgenic lines were generated as follows. The *PHOT1*^{I608E} mutated cDNA was generated from *PHOT1* cDNA by PCR-based site-directed mutagenesis using *PHOT1*-gene specific primers including 5'-ACTGCAGTTTTTTCACCAGGTCTTCTCCCTC-3' and 5'-ACTGCAGTGAATGAAGATGAAGCGGTTCGAGAACT-3' (underlined bases denote the Glu [E] codon 608; double underlines indicate the PstI sites for subsequent subcloning), subcloned into the entry vector pDONR222 (Invitrogen), and shuttled into pMDC7 via an LR clonase reaction. The *pMDC7-PHOT1*^{I608E} plasmid was used for the transformation of *A. tumefaciens*, which was then used

529 for subsequent transformations of *phot1*-Salk146058 mutants.

530 The *35Spro:UBQ3* transgenic lines were generated as follows. The
531 POLYUBIQUITIN 3 (UBQ3) coding region was amplified from Col genome DNA
532 by PCR using *UBQ3*-gene specific primers (Supplemental Table S1), subcloned
533 into the entry vector pENTR/D-TOPO, and shuttled via an LR clonase reaction
534 into the cauliflower mosaic virus 35S promoter-containing binary vector pH35GS,
535 which was kindly provided by Professor Taku Demura (Nara Institute of Science
536 and Technology, Nara, Japan). The resulting *pH35GS-UBQ3* plasmid was used
537 for the transformation of *A. tumefaciens*, which was then used for subsequent
538 transformations of wild type (Col) plants.

539 For experiments, the seeds were surface-sterilized and plated in Petri
540 dishes with half-strength Okada and Shimura medium containing 1.5% agar, as
541 described previously (Ohgishi et al., 2004). Seeds were kept at 4°C for 3 days
542 and then exposed to red light for 6 h to induce uniform germination. After
543 germination was induced, the Petri dishes were positioned vertically to let the
544 seedlings grow on the surface of the agar at 21 to 22°C under dark conditions.
545 Blue-light and red-light irradiations were performed under various conditions with
546 light-emitting diodes (Ohgishi et al., 2004), as described in the Figure legends.

547

548 **Yeast Two-Hybrid Analysis**

549 The GAL4 DNA-binding domain vector pGBDKT7-GWRFC was constructed by
550 insertion of the Gateway reading frame cassette RfcC (Invitrogen) into the

Klenow-Fragment-treated NdeI-SalI sites of pGBKT7 (pGBDKT7: Clontech, http://www.clontech.com). PCR was used to generate the coding sequences of PHOT1 and PHOT2 with gene specific primers (Supplemental Table S1). A DNA fragment for PHOT1 N2mut was separately generated by PCR using N2 FW and N2mut RV and N2mut FW and N2 RV primers, and then combined by PCR using N2 FW and N2 RV primers. These amplified products were subcloned into the entry vector pENTR/D-TOPO and shuttled into the pGBDKT7-GWRFC plasmid. The GAL4 transcription-activating domain vector pGADT7 and its derivative pGADT7-RPT2 N were prepared as described previously (Inada et al., 2004). Pairwise combinations of vectors were co-transformed into the yeast strain Y187 (Clontech) and plated onto the same selective medium. Quantitative β-galactosidase assays were performed in liquid cultures of yeast using *o*-nitrophenyl-β-D-galactopyranoside (Ausubel et al., 2001). One unit of β-Gal activity was defined as the amount of enzyme required to convert 1 μmol of *o*-nitrophenyl-β-D-galactopyranoside to *o*-nitrophenol and D-galactose in 1 min at 30°C.

In vitro Pull-Down Assay

To prepare phot1 LOV1 and LOV2 proteins, DNA fragments for *PHOT1 N2* and *N4* in pENTR/D-TOPO (Invitrogen) were transferred into the pCold ProS2 plasmid (TaKaRa) harboring a gateway reading flame cassette (Invitrogen). These constructs were introduced into *Escherichia coli* strain BL21 (DE3) pLysS

573 (Novagen), and His-ProS-tagged PHOT1 N2 and N4 proteins (His-PHOT1N2
574 and –PHOT1N4) were prepared from the transformed lines in accordance with
575 the manufacturer's protocol. HA-tagged RPT2 N proteins were prepared with *in*
576 *vitro* transcription and translation of pGADT7-RPT2 N using the TNT Quick
577 Coupled Transcription/Translation Systems (Promega).

578 Each purified protein preparation of His-PHOT1 N2 and N4 was
579 incubated with TALON Magnetic Beads (TaKaRa) at 4°C for 30 min and further
580 incubated at 4°C for 30 min with *in vitro* transcription and translation reactant
581 containing RPT2 N. The beads were then collected on the magnetic rack and
582 washed five times with washing buffer (sodium phosphate buffer pH 7.0, 150 mM
583 NaCl, 0.2% Triton-X100). The proteins were then released from the beads into 50
584 µL of 1× SDS gel loading buffer and resolved by SDS-PAGE.

585

586 **Immunoblotting Analysis**

587 For immunoblotting of Phos-tag SDS-PAGE gels, total proteins were extracted
588 from etiolated seedlings in a buffer containing 50 mM Tris-MES, pH 7.5, 300 mM
589 sucrose, 150 mM NaCl, 10 mM potassium acetate, 0.2% Triton X-100, and a
590 protease inhibitor mixture (Complete Mini EDTA-free; Roche Diagnostics). The
591 extracts were then centrifuged at 10,000 g at 4°C for 10 min to remove cell debris
592 and the supernatants were collected and mixed with a half volume of 3× SDS gel
593 loading buffer, and boiled at 95°C for 15 min. The samples were separated with
594 6% SDS-PAGE gels containing 2 µM Phos-tag (FUJIFILM Wako Pure Chemical

595 Corporation) in accordance with the previously described "Zn^{2+}-Phos-tag SDS
596 PAGE" method (Kinoshita and Kinoshita-Kikuta, 2011). Following
597 electrophoresis, the gels were twice washed with methanol-free transfer buffer
598 (25 mM Tris, 192 mM glycine) with 10 mM EDTA for 10 min and then once with
599 methanol-free transfer buffer without EDTA for 10 min. The separated total
600 proteins were then blotted onto a PVDF membrane using a wet tank blotting
601 system at a constant voltage of 350 mA for 4 h. Later immunoblotting steps were
602 performed as described previously (Inada et al., 2004). For alkaline phosphatase
603 treatment, microsomal pellets were obtained as described previously (Inada et
604 al., 2004) and resuspended in the 1× NEBuffer 3 (NEB) with 0.5% Triton-X100
605 and protease inhibitor mixture (Complete Mini EDTA-free; Roche Diagnostics).
606 30 μg of microsomal proteins were then treated with 30 units of calf intestinal
607 alkaline phosphatase (TaKaRa) at 37°C for 2 h. The reaction was stopped adding
608 3× SDS gel loading buffer.

609 For immunoblotting of SDS-PAGE gels without Phos-tag, total proteins
610 were extracted, separated on 6, 7.5, or 10% SDS-PAGE gels, and blotted onto
611 PVDF membranes, as described previously (Inada et al., 2004). Anti-RPT2,
612 anti-PHOT1, and horseradish peroxidase (HRP)-conjugated anti-rabbit IgG
613 antibodies were prepared as described previously (Haga et al., 2015).
614 Anti-PHOT2 antiserum was produced in rabbit using 10× His-tagged PHOT2
615 products incorporating residues 294-474 as the antigen. HRP activity was
616 detected with the super-signal west femto maximum sensitivity substrate

(Thermo Scientific) and the Image Quant LAS4000 Mini device (GE Healthcare). As a loading control, the protein-blotted membranes were stained using the Pierce reversible protein staining kit (Thermo Scientific). The results were confirmed using independent samples. For the statistical analysis, the signal intensities of the protein bands were quantified with Fiji software (Schindelin et al., 2012).

In vitro Phosphorylation Assay

In vitro phosphorylation assays of a 120-kDa protein in microsomal membranes were performed as described previously (Sakai et al., 2000), with some modifications. Briefly, microsomal membrane pellets were obtained from approximately 650 two-day-old etiolated transgenic seedlings of *pMDC7-PRT2* and *pER8,* which were grown on the half-strength OS agar medium with or without 10 μM estradiol. The pellets were resuspended in 30 μL of phosphorylation buffer (50 mM Tris-MES, pH 7.5, 5 mM MgSO4, 150 mM NaCl, 1 mM EGTA, 1 mM DTT, 0.5% Triton X-100, and a protease inhibitor mixture [Complete Mini EDTA-free; Roche Diagnostics]) by pipetting. All manipulations were performed at 4°C under a dim red safelight.

Twenty micrograms of microsomal extract were diluted to a final volume of 9 μL in phosphorylation buffer and γ-^{32}P-ATP was added to a final concentration of 200 μM (specific activity, 2.5 Ci/mmol). The membrane extracts were then incubated for 2 min at 30°C and irradiated with blue light at 10 μmol m^{-}

639 ^{2} s^{-1} for 16 min. Dark control samples were mock-irradiated. After the irradiations,
640 the samples were mixed with an equal volume of 2× SDS gel loading buffer to
641 stop the reaction. Ten micrograms of each sample were then electrophoresed on
642 an a 6% SDS–PAGE gel. Gels were dried and then autoradiographed by
643 exposure to X-ray film. The images of these films were recorded with a scanner
644 (ES8500; Epson) and the signal intensities of the 120 kDa protein were quantified
645 with Fiji software (Schindelin et al., 2012).
646
647 **Treatments of Protein Phosphatase Inhibitors**
648 Cantharidin and okadaic acid (CN and OKA: Fujifilm Wako) were prepared as 50
649 mM and 1 mM stock solutions, respectively, in dimethyl sulfoxide (DMSO). The
650 treatments with these chemicals were performed as described previously
651 (Sullivan et al., 2019) with brief modifications. Briefly, the aerial portions of the
652 hypocotyls were prepared from two-day-old etiolated seedlings with a blade
653 under safe green light conditions. Red light-irradiation at 10 μmol m^{-2} s^{-1} for 2 min
654 was performed prior to preparation of the segment. The segments were then
655 dipped in half strength OS solution containing 30 μM CN, 1 μM OKA or an
656 equivalent volume of DMSO and vacuum infiltrated for 15 min. After a
657 subsequent incubation under darkness for 105 min at 60 rpm, the segments were
658 irradiated with blue light at 0.1 μmol m^{-2} s^{-1} for 30 min, immediately harvested
659 with forceps, and frozen with liquid nitrogen.
660

661 **GUS Histochemical Analysis**

662 Transgenic seedlings carrying the *RPT2pro:GUS* gene were stained with
663 5-bromo-4-chloro-3-indolyl-β-glucuronide (X-Gluc), as described previously
664 (Nagashima et al., 2008). Seedling images were obtained with an MZ-16FA
665 /DFC500 digital stereomicroscope (Leica, http://www.leica-microsystems.com).

666

667 **VENUS Imaging**

668 VENUS fluorescence was visualized with an MZ-16FA/DFC500 digital
669 stereomicroscope with the YFP filter (Leica). Confocal fluorescence images were
670 recorded as described previously (Haga et al., 2015). The VENUS signal
671 intensity was quantified with Fiji software (Schindelin et al., 2012). To prepare
672 hypocotyl cross sections, the *rpt2* mutant transformed with a
673 *RPT2pro:RPT2-VENUS* gene were irradiated with blue light at 10 μmol m^{-2} s^{-1}
674 for 6 h, subsequently mounted in 2% agarose and hand-sectioned with a blade.

675

676 **Transcriptional Analysis by qRT-PCR**

677 Total RNA was extracted using a RNeasy kit (QIAGEN). Quantitative RT-PCR
678 was carried out using a PCR system (StepOne; Applied Biosystems) and the
679 Luna One-Step RT-qPCR Kit (NEB) in accordance with the manufacturer's
680 protocol. Triplicate PCR reactions were performed in each case and three
681 biological independent samples were used for each gene. The primers used are
682 listed in Supplemental Table S2 and *18S rRNA* was amplified as an internal

683 standard.

684

685 **Measurement of Phototropic Curvature**

686 Phototropic curvatures of hypocotyls were measured on agar medium in 0.2 ml

687 tubes using the “advanced method” described previously (Haga et al. 2012; Haga

688 and Kimura, 2019).

689 **Accession Numbers**

690 The sequence data for this article can be found in the Arabidopsis Genome
691 Initiative or the EMBL/GenBank data libraries under the following accession
692 numbers: *RPT2* (AT2G30520), *PHOT1* (AT3G45780), *NPH3* (AT5G64330),
693 *PHOT2* (AT5G58140) and *UBQ3* (AT5G03240).

694

695 **Supplemental Data**

696

697 **Supplemental Figure 1.** Time course analysis of continuous light-induced
698 phototropism in the *phot1 phot2* double mutants transformed with a
699 *35Spro:PHOT1*^{LOV1Cys39Ala} gene.

700

701 **Supplemental Figure 2.** Time course analysis of phot1 autophosphorylation in
702 tube-grown seedlings.

703

704 **Supplemental Figure 3.** The effect of phosphatase on the *rpt2*-induced mobility
705 shift of PHOT1 during Phos-tag SDS-PAGE.

706

707 **Supplemental Figure 4.** Evaluation of anti-PHOT2 antibody.

708

709 **Supplemental Figure 5.** Binding activity of phot2 to RPT2.

710

711 **Supplemental Figure 6.** Characterization of the *rpt2* mutants transformed with a
712 *pMDC7-RPT2* construct.
713
714 **Supplemental Figure 7.** Suppression of phot1 dephosphorylation by protein
715 phosphatase inhibitors.
716
717 **Supplemental Figure 8.** Effect of the proteasome inhibitor MG132 on RPT2
718 protein expression in wild-type seedlings under red light conditions.
719
720 **Supplemental Figure 9.** Phenotypes of the *35Spro:UBQ3* transgenic lines.
721
722 **Supplemental Table 1.** Gene-specific primers used for construction.
723
724 **Supplemental Table 2.** Gene-specific primers used for qRT-PCR.
725
726 **Acknowledgments**
727 We thank the Arabidopsis Biological Resource Center for providing the *phot1*
728 (Salk146058) and *phot2* (Salk142275) seeds. We also thank Professor John
729 Christie (University of Glasgow, Glasgow, UK) for kindly providing the seeds of
730 the *35Spro:PHOT1*^{LOV1C39A} transgenic line, Professor Nam-Hai Chua
731 (Rockefeller University, New York, NY) for generously donating the pMDC7
732 vector, and Dr. Masatoshi Yamaguchi (Saitama University, Saitama, Japan) and

Professor Taku Demura (Nara Institute of Science and Technology) for generously supplying the pH35GS binary vectors. This work was supported by the Japan Society for the Promotion of Science (KAKENHI 22570058, 25120710, 16H01231, 17H03694, 18K19329 to T.S.).

Author Contributions

T.K, T.T.-M. and T.S. designed and conducted most of the research, and analyzed the data. H.I., K.O. and K.I. designed and performed the phot1 in vitro phosphorylation assay. T.K. and T.S. wrote the article.

REFERENCES

Alonso, J.M., Stepanova, A.N., Leisse, T.J., Kim, C.J., Chen, H., Shinn, P., Stevenson, D.K., Zimmerman, J., Barajas, P., Cheuk, R., Gadrinab, C., Heller, C., Jeske, A., Koesema, E., Meyers, C.C., Parker, H., Prednis, L., Ansari, Y., Choy, N., Deen, H., Geralt, M., Hazari, N., Hom, E., Karnes, M., Mulholland, C., Ndubaku, R., Schmidt, I., Guzman, P., Aguilar-Henonin, L., Schmid, M., Weigel, D., Carter, D.E., Marchand, T., Risseeuw, E., Brogden, D., Zeko, A., Crosby, W.L., Berry, C.C., and Ecker, J.R. (2003). Genome-Wide Insertional Mutagenesis of *Arabidopsis thaliana*. *Science* 301: 653-657.

Ausubel, F.M., Brent, R., Kingston, R.E., Moore, D.D., Seidman, J.G., Smith, J.A., and Struhl, K. (2001). Current Protocols in Molecular Biology. New York, NY: John Wiley & Sons.

Casal, J.J., Candia, A.N., and Sellaro, R. (2014). Light perception and signaling by phytochrome A. *Journal of Experimental Botany* 65: 2835-2845.

Christie, J.M., Reymond, P., Powell, G.K., Bernasconi, P., Raibekas, A.A., Liscum, E., and Briggs, W.R. (1998). *Arabidopsis* NPH1: a flavoprotein with the properties of a photoreceptor for phototropism. *Science* 282: 1698-1701.

Christie, J.M., Swartz, T.E., Bogomolni, R.A., and Briggs, W.R. (2002). Phototropin LOV domains exhibit distinct roles in regulating photoreceptor function. *The Plant Journal* 32: 205-219.

Christie, J.M. (2007). Phototropin blue-light receptors. *The Annual Review of Plant Biology* 58: 21-45.

765 Clough, R.C., and Vierstra, R.D. (1997). Phytochrome degradation. *Plant, Cell &*
766 *Environment* 20: 713-721.
767 Curtis, M.D., and Grossniklaus, U. (2003). A gateway cloning vector set for
768 high-throughput functional analysis of genes in planta. *Plant Physiol*
769 133:462-469.
770 de Wit, M., Galvão, V.C., and Fankhauser, C. (2016). Light-Mediated Hormonal
771 Regulation of Plant Growth and Development. *Annual Review of Plant Biology*
772 67: 513-537.
773 Genschik, P., Sumara, I., and Lechner, E. (2013). The emerging family of
774 CULLIN3-RING ubiquitin ligases (CRL3s): cellular functions and disease
775 implications. *The EMBO Journal* 32: 2307-2320.
776 Haga, K., and Kimura, T. (2019). Physiological Characterization of Phototropism
777 in *Arabidopsis* seedlings. In *Method in Molecular Biology 1924 Phototropism*,
778 Yamamoto, K. T. ed (New York, USA: Human Press), pp. 3-17.
779 Haga, K., and Sakai, T. (2012). PIN auxin efflux carriers are necessary for
780 pulse-induced but not continuous light-induced phototropism in Arabidopsis.
781 *Plant Physiol.* 160: 763-776.
782 Haga, K., Tsuchida-Mayama, T., Yamada, M., and Sakai, T. (2015). Arabidopsis
783 ROOT PHOTOTROPISM2 Contributes to the Adaptation to High-Intensity
784 Light in Phototropic Responses. *The Plant Cell.* 27: 1098-1112.
785 Harada, A., Takemiya, A., Inoue, S., Sakai, T., and Shimazaki, K. (2013). Role of
786 RPT2 in leaf positioning and flattening and a possible inhibition of phot2

787 signaling by phot1. *Plant & Cell Physiology* 54: 36-47.

788 Harper, S.M., Christie, J.M., and Gardner, K.H. (2004). Disruption of the LOV-Jα
789 helix interaction activates phototropin kinase activity. *Biochemistry* 43:
790 16184-16192.

791 Inada, S., Ohgishi, M., Mayama, T., Okada, K., and Sakai, T. (2004). RPT2 is a
792 signal transducer involved in phototropic response and stomatal opening by
793 association with phototropin 1 in *Arabidopsis thaliana*. *The Plant Cell* 16:
794 886-897.

795 Kagawa, T., Sakai, T., Suetsugu, N., Oikawa, K., Ishiguro, S., Kato, T., Tabata,
796 S., Okada, K., and Wada, M. (2001). *Arabidopsis* NPL1: a phototropin
797 homolog controlling the chloroplast high-light avoidance response. *Science*
798 291: 2138-2141.

799 Kaiserli, E., Sullivan, S., Jones, M.A., Feeney, K.A., and Christie, J.M. (2009).
800 Domain swapping to assess the mechanistic basis of Arabidopsis phototropin
801 1 receptor kinase activation and endocytosis by blue-light. *Plant Cell*. 21:
802 3226-3244.

803 Kinoshita, T., Doi, M., Suetsugu, N., Kagawa, T., Wada, M., and Shimazaki, K.
804 (2001). Phot1 and phot2 mediate blue light regulation of stomatal opening.
805 *Nature* 414: 656-660.

806 Kinoshita, E., and Kinoshita-Kikuta, E. (2011). Improved Phos-tag SDS-PAGE
807 under neutral pH conditions for advanced protein phosphorylation profiling.
808 *Proteomics* 11: 319-323.

809 Li, J., Li, G., Wang, H., and Deng, X.Q. (2011). Phytochrome signaling
810 mechanism. *The Arabidopsis Book* e0148.
811 Lin, C., Yang, H., Guo, H., Mockler, T., Chen, J., and Cashmore, A.R. (1998).
812 Enhancement of blue-light sensitivity of Arabidopsis seedlings by a blue light
813 receptor cryptochrome 2. *Proceedings of the National Academy of Sciences of*
814 *the United States of America* 95: 2686-2690.
815 Liscum, E., and Briggs, W.R. (1995). Mutations in the *NPH1* locus of Arabidopsis
816 disrupt the perception of phototropic stimuli. *The Plant Cell* 7: 473-485.
817 Motchoulski, A., and Liscum, E. (1999). *Arabidopsis* NPH3: A NPH1
818 photoreceptor-interacting protein essential for phototropism. *Science* 286:
819 961-964.
820 Nagashima, A., Suzuki, G., Uehara, Y., Saji, K., Furukawa, T., Koshiba, T.,
821 Sekimoto, M., Fujioka, S., Kuroha, T., Kojima, M., Sakakibara, H., Fujisawa,
822 N., Okada, K., and Sakai, T. (2008). Phytochromes and cryptochromes
823 regulate the differential growth of Arabidopsis hypocotyls in both a
824 PGP19-dependent and -independent manner. *The Plant Journal* 53, 516-529.
825 Nakasako, M., Iwata, T., Matsuoka, D., and Tokutomi, S. (2004). Light-induced
826 structural changes of LOV domain-containing polypeptides from *Arabidopsis*
827 phototropin 1 and 2 studied by small-angle X-ray scattering. *Biochemistry* 43:
828 14881-14890.
829 Ohgishi, M., Saji, K., Okada, K., and Sakai, T. (2004). Functional analysis of each
830 blue-light receptor, cry1, cry2, phot1, and phot2, by using combinatorial

831 multiple mutants in Arabidopsis. *Proceedings of the National Academy of*
832 *Sciences of the United States of America* 101: 2223-2228.
833 Okajima, K., Kashojiya, S., and Tokutomi, S. (2012). Photosensitivity of kinase
834 activation by blue-light involves the lifetime of a cysteinyl-flavin adduct
835 intermediate, S390, in the photoreaction cycle of the LOV2 domain in
836 phototropin, a plant blue-light receptor. *Journal of Biological Chemistry* 287:
837 40972-40981.
838 Okajima, K. (2016). Molecular mechanism of phototropin light signaling. *Journal*
839 *of Plant Research* 129: 159-166.
840 Pedmale, U.V., and Liscum, E. (2007). Regulation of phototropic signaling in
841 *Arabidopsis* via phosphorylation state changes in the phototropin 1-interacting
842 protein NPH3. *Journal of Biological Chemistry* 282: 19992-20001.
843 Petersen, J., Inoue, S.I., Kelly, S.M., Sullivan, S., Kinoshita, T., and Christie, J.M.
844 (2017). Functional characterization of a constitutively active kinase variant of
845 *Arabidopsis* phototropin 1. *Journal of Biological Chemistry* 292: 13843-13852.
846 Rademacher, E.H., and Offringa, R. (2012). Evolutionary Adaptations of Plant
847 AGC Kinases: From Light Signaling to Cell Polarity Regulation. *Frontiers in*
848 *Plant Science* 3: 250.
849 Roberts, D., Pedmale, U.V., Morrow, J., Sachdev, S., Lechner, E., Tang, X.,
850 Zheng, N., Hannink, M., Genschik, P., and Liscum, E. (2011). Modulation of
851 phototropic responsiveness in *Arabidopsis* through ubiquitination of
852 phototropin 1 by the CUL3-Ring E3 ubiquitin ligase CRL3 (NPH3). *The Plant*

853 *Cell* 23: 3627-3640.

854 Sakai, T., Wada, T., Ishiguro, S., and Okada, K. (2000). RPT2. A signal
855 transducer of the phototropic response in Arabidopsis. *The Plant Cell* 12:
856 225-236.

857 Sakai, T., Kagawa, T., Kasahara, M., Swartz, T.E., Christie, J.M., Briggs, W.R.,
858 Wada, M., and Okada, K. (2001). *Arabidopsis* nph1 and npl1: blue-light
859 receptors that mediate both phototropism and chloroplast relocation.
860 *Proceedings of the National Academy of Science of America* 98: 6969-6974.

861 Sakai, T. (2005). NPH3 and RPT2: signal transducers in phototropin signaling
862 pathways. In *Light Sensing in Plants*, Wada M, Shimazaki K, Iino M eds
863 (Tokyo, Japan: Springer-Verlag), pp. 179-184.

864 Sakamoto, K., and Briggs, W.R. (2002). Cellular and subcellular localization of
865 phototropin 1. *The Plant Cell* 14: 1723-1735.

866 Schindelin, J., Arganda-Carreras, I., Frise, E., Kaynig, V., Longair, M., Pietzsch,
867 T., Preibisch, S., Rueden, C., Saalfeld, S., Schmid, B., et al. (2012) Fiji: An
868 open-source platform for biological-image analysis. *Nat Methods* 9: 676–68

869 Sharrock, R.A., and Clack, T. (2002). Patterns of expression and normalized
870 levels of the five Arabidopsis phytochromes. *Plant Physiology* 130: 442-456.

871 Sullivan, S., Thomson, C.E., Lamont, D.J., Jones, M.A., and Christie, J.M.
872 (2008). In vivo phosphorylation site mapping and functional characterization of
873 Arabidopsis phototropin 1. *Molecular Plant* 1: 178-194.

874 Sullivan, S., Kharshiing, E., Laird, J., Sakai, T., and Christie, J.M. (2019).

875 Deetiolation Enhances Phototropism by Modulating NON-PHOTOTROPIC
876 HYPOCOTYL3 Phosphorylation Status. *Plant Physiology* 180: 1119-1131.
877 Suetsugu, N., Takemiya, A., Kong, S.G., Higa, T., Komatsu, A., Shimazaki, K.,
878 Kohchi, T., and Wada, M. (2016). RPT2/NCH1 subfamily of NPH3-like proteins
879 is essential for the chloroplast accumulation response in land plants.
880 *Proceedings of the National Academy of Science of America* 113:
881 10424-10429.
882 Suzuki, H., Koshiba, T., Fujita, C., Yamauchi, Y., Kimura, T., Isobe, T., Sakai, T.,
883 Taoka, M, and Okamoto, T. (2019). Low-fluence blue light-induced
884 phosphorylation of Zmphot1 mediates the first positive phototropism. *Journal*
885 *of Experimental Botany* in press.
886 Tsuchida-Mayama, T., Nakano, M., Uehara, Y., Sano, M., Fujisawa, N., Okada,
887 K., and Sakai, T. (2008). Mapping of the phosphorylation sites on the
888 phototropic signal transducer, NPH3. *Plant Science* 174: 626-633.
889 Tsuchida-Mayama, T., Sakai, T., Hanada, A., Uehara, Y., Asami, T., and
890 Yamaguchi, S. (2010). Role of the phytochrome and cryptochrome signaling
891 pathways in hypocotyl phototropism. *The Plant Journal* 62: 653-662.
892 Xue, Y., Xing, J., Wan, Y., Lv, X., Fan, L., Zhang, Y., Song, K., Wang, L., Wang,
893 X., Deng, X., Baluška, F., Christie, J.M., and Lin, J. (2018). *Arabidopsis*
894 Blue-light Receptor Phototropin 1 Undergoes Blue-light-Induced Activation in
895 Membrane Microdomains. *Molecular Plant* 11: 846-859.
896 Zuo, J., Niu, Q.W., and Chua, N.H. (2000). An estrogen receptor-based

897 transactivator XVE mediates highly inducible gene expression in transgenic

898 plants. *The Plant Journal* 24: 265-273.

899

900 **Figure legends**

901

902 **Figure 1.** Interaction between phot1 and RPT2.

903 **(A)** Schematic representation of the phot1 structure. The Ser/The protein kinase
904 and LOV domains are denoted by the solid and dotted blocks, respectively. The
905 amino acid residues used for each underlined construct are indicated in
906 parentheses.

907 **(B)** Yeast two-hybrid assay of phot1–RPT2 interactions. Solution assays of
908 β-galactosidase (β-Gal) activity were performed for the combinations indicated on
909 the left. The data shown are mean values ± SE (n = 3). The asterisk denotes
910 statistically significant differences compared with the vector control (Student's t
911 test; $P < 0.05$).

912 **(C)** In vitro pull-down assay to verify the interaction between the LOV domains of
913 phot1 and the N-terminal half of RPT2. HA-tagged proteins of the N-terminal half
914 of RPT2 (HA-RPT2 N) were incubated with the His-tagged LOV1 or LOV2
915 domains of phot1 for the His-tag pull-down assay and detected by
916 immunoblotting using an anti-HA (α-HA) antibodies. HA-RPT2 N proteins without
917 pull down were also electrophoresed as a control (Input). The protein-blotted
918 membrane was stained using a Pierce reversible protein staining kit.

919

920 **Figure 2.** RPT2 suppresses the autophosphorylation of phot1.

921 **(A)** Immunoblotting analysis of PHOT1 in wild type (Col) and *rpt2* mutant

Arabidopsis. Two-day-old etiolated seedlings were irradiated with unilateral blue light at the indicated fluence rates for 2 h. Total proteins (20 μg) extracted from the seedlings were separated on 6% SDS-PAGE gels with 2 μM Phos-tag (+ Phos-tag), followed by immunoblotting with anti-PHOT1 (α-PHOT1) antibodies. 10 μg of the total proteins were separated on 6% SDS-PAGE gels without Phos-tag (– Phos-tag) for comparison. An asterisk indicates a non-specific band. The protein-blotted membranes were stained as a loading control.

(B and C) Time courses analysis of phot1 autophosphorylation. Two-day-old etiolated seedlings were irradiated with unilateral blue light at 100 μmol m^{-2} s^{-1} in **(B)** or 0.1 μmol m^{-2} s^{-1} in **(C)** for the indicated times. Other details are as described in **(A)**.

(D) Immunoblotting analysis of PHOT2 in wild type (Col) and *rpt2* mutant. Immunoblotting was performed with an anti-PHOT2 (α-PHOT2) antibodies. Other details were as in **(A)**.

(E) Time course analysis of phot2 autophosphorylation. Two-day-old etiolated seedlings were irradiated with unilateral blue light at 100 μmol m^{-2} s^{-1} for the indicated times. Immunoblotting was performed with α-PHOT2 and anti-RPT2 (α-RPT2) antibodies. Other details are as described in **(A).**

(F) Autophosphorylation of phot1 and phot2 in the *rpt2* mutants transformed with a *35Spro:RPT2* gene (*35Spro:RPT2*). Two-day-old etiolated seedlings were irradiated with unilateral blue light at 100 μmol m^{-2} s^{-1} for 30 minutes. Immunoblotting was performed with α-PHOT1, α-PHOT2 and α-RPT2

antibodies. Other details are as described in **(A)**.

Figure 3. In vitro blue light-induced phosphorylation of a 120-kDa protein in microsomal membranes.

Two-day-old etiolated *rpt2* mutants transformed with a *pMDC7-RPT2* construct (*pMDC7-RPT2*) or wild-type seedlings transformed with a *pER8* vector control (*pER8*) were grown on agar medium with (–) or without (+) 10 μM estradiol (Est) under darkness. Microsomal proteins were then extracted.

(A) In vitro blue light-induced phosphorylation of a 120-kDa protein in microsomal membranes. Microsomal proteins were irradiated with mock (BL –) or blue light (BL +) at 10 μmol m^{-2} s^{-1} for 16 min in the presence of γ-^{32}P-ATP. The reacted samples were resolved on 6% SDS-PAGE gels and autoradiographed.

(B) Relative quantity of phosphorylated 120-kDa proteins. The value was calculated against the data from Est-untreated, blue light-irradiated *pMDC7-RPT2* seedlings. The data shown are mean values ± SE (n = 3). An asterisk indicates a statistically significant difference (Student's t test; $P < 0.05$).

Figure 4. Effects of protein phosphatase inhibitors on the phosphorylation status of phot1.

The aerial parts of two-day-old etiolated seedlings were incubated under darkness for 2 h in liquid medium with a protein phosphatase inhibitor (PPase inhibitor), 30 μM cantharidin (CN) or 1 μM okadaic acid (OKA), and subsequently

966 treated with blue light at 0.1 μmol m^{-2} s^{-1} for 0.5 h. Total proteins (15 μg for **A**, 20
967 μg for **B**) extracted from the seedlings were separated on 6% SDS-PAGE gels
968 with 2 μM Phos-tag, followed by immunoblotting with α-PHOT1 antibodies.
969 Protein-blotted membranes were stained as a loading control.
970 **(A)** Effects of PPase inhibitors on the aerial parts of wild-type (Col) seedlings and
971 *rpt2* mutants. Red light pretreatments were conducted to induce RPT2
972 expression before exposure to the PPase inhibitor.
973 **(B)** Effects of PPase inhibitors on the aerial parts of wild-type (Col) seedlings and
974 the *35Spro:RPT2* lines (OX).
975
976 **Figure 5.** Expression patterns of the *RPT2pro:GUS* and the
977 *RPT2pro:RPT2-VENUS* genes.
978 Two-day-old etiolated seedlings were mock-irradiated **(**Mock: **A, D, G, J, M, P)**,
979 or red light- **(**RL: **B, E, H, K, N, Q)** or blue light- **(**BL: **C, F, I, L, O, R)** irradiated at
980 10 μmol m^{-2} s^{-1} for 4 h. Scale bars: 1.0 mm **(A-C, J-L)**; 400 μm **(D-F, M-O)**; 100
981 μm **(G-I, P-R)**.
982 **(A-I)** GUS staining patterns of wild-type seedlings transformed with a
983 *RPT2pro:GUS* gene.
984 **(J-R)** VENUS fluorescent images of the *rpt2* mutants transformed with a
985 *RPT2pro:RPT2-VENUS* gene.
986 **(S)** Signal intensities of RPT2-VENUS fluorescence. Fluorescent signals were
987 measured in the upper region of the hypocotyls and calculated relative to the

988 value from BL-irradiated seedlings. The data shown are the mean values ± SE
989 from 9 seedlings. Asterisks indicate a statistically significant difference (Student's
990 t test; $P < 0.01$).
991
992 **Figure 6.** Post-transcriptional regulation of RPT2 expression by phototropins.
993 **(A)** Immunoblotting analysis of RPT2 proteins in wild type (Col), *phot1* and *nph3*
994 seedlings. Two-day-old etiolated seedlings were mock-irradiated (Mock), or red
995 light- (RL) or blue light- (BL) irradiated at 10 μmol m^{-2} s^{-1} for 6 h. Total proteins
996 (10 μg) extracted from the seedlings were resolved on 10% SDS-PAGE gels,
997 followed by immunoblotting with α-RPT2 antibodies. The protein-blotted
998 membranes were stained as a loading control.
999 **(B)** Statistical analysis of the data in **(A)**. The values were normalized with a
1000 loading control and then calculated against the data from the blue light-irradiated
1001 seedlings of wild type. The data shown are mean values ± SE ($n = 3$). Asterisks
1002 indicate a statistically significant difference (Student's t test; $P < 0.05$).
1003 **(C)** qRT-PCR analysis of *RPT2* in wild type (Col), *phot1* and *nph3* seedlings.
1004 Two-day-old etiolated seedlings were irradiated with blue light at 10 μmol m^{-2} s^{-1}
1005 for 6 h or mock-irradiated. The values were normalized using an internal control
1006 (*18S rRNA*) and then calculated against the values from blue light-irradiated
1007 seedlings of wild type. The data shown are the mean values ± SE ($n = 3$).
1008 **(D)** Immunoblotting analysis of PHOT1, RPT2 and NPH3 in the *phot1* mutants
1009 transformed with a *pMDC7-PHOT1*^{I608E} construct (*pMDC7-PHOT1*^{I608E}: two

1010 independent lines, #1 and #2) and the *pER8* vector control line. Two-day-old
1011 etiolated seedlings were grown on agar medium with (+) or without (–) 10 μM
1012 estradiol (Est). Microsomal proteins (7.5 μg) extracted from the seedlings were
1013 separated on 7.5% SDS-PAGE gels, followed by immunoblotting with α-PHOT1,
1014 α-RPT2 and anti-NPH3 (α-NPH3) antibodies. The protein-blotted membranes
1015 were stained as a loading control.
1016 **(E)** Fluence-rate dependency of the RPT2 induction in wild type (Col), *phot1* and
1017 *phot1 phot2* double mutants. Two-day-old etiolated seedlings were irradiated with
1018 blue light at the indicated fluence rate for 6 h. Other details were as described in
1019 **(A)**.
1020 **(F)** Time course analysis of RPT2 induction in wild type (Col) and *phot1*
1021 seedlings. Two-day-old etiolated seedlings were irradiated with blue light at 0.1
1022 (left panel) or 10 μmol m^{-2} s^{-1} (right panel) for the indicated period. Other details
1023 were as described in **(A).**
1024 **(G)** Statistical analysis of the data generated in **(F)**. The values were normalized
1025 using a loading control and then calculated against the values from wild-type
1026 seedlings irradiated for 2 h. The data shown are mean values ± SE (n = 3).
1027 Asterisks indicate a statistically significant difference (Student's t test; $P < 0.05$).
1028
1029 **Figure 7.** Distribution patterns of the RPT2-VENUS proteins in etiolated
1030 hypocotyls.
1031 Two-day-old etiolated seedlings of the *rpt2* mutants transformed with a

1032 *RPT2pro:RPT2-VENUS* gene were irradiated with blue light (BL) at 10 μmol m^{-2}
1033 s^{-1} for 6 h from above **(A)** or for 2 h from the unilateral side **(B)**.
1034 **(A)** A typical distribution pattern of RPT2-VENUS in the hypocotyl cross section.
1035 H, hypocotyl; C, cotyledon.
1036 **(B and C)** Distribution patterns of RPT2-VENUS in the upper region of the
1037 hypocotyls. Distribution patterns were classified into three types (Irradiated side,
1038 Even and Shaded side). Representative confocal (left panel), bright field (mid
1039 panel) and merged images (right panel) are shown in **(B)**. Arrows indicate the
1040 direction of blue light. The frequencies of each expression pattern were
1041 calculated from 74 seedlings and are shown in **(C)**. White bar, 100 μm.
1042
1043 **Figure 8.** Destabilization of the RPT2 protein via a ubiquitin-proteasome
1044 dependent pathway.
1045 **(A)** Effect of the proteasome inhibitor MG132 on RPT2 protein expression.
1046 Two-day-old etiolated seedlings of wild type (Col) and *phot1 phot2* double mutant
1047 were transferred into liquid medium with (+) or without (–) 50 μM MG132, kept in
1048 the dark for 1 h, and subsequently irradiated with blue light (BL) at 10 μmol m^{-2} s^{-}
1049 ^{1} for 3 h (+) or mock-irradiated (–). Total proteins (10 μg) extracted from the
1050 seedlings were separated on 7.5% SDS-PAGE gels, followed by immunoblotting
1051 with α-RPT2 antibodies. The protein-blotted membranes were stained as a
1052 loading control.
1053 **(B)** Immunoblotting analysis of RPT2, PHOT1, PHOT2 and NPH3 in wild-type

(Col) seedlings and wild-type seedlings transformed with *35Spro:UBQ3* (*35Spro:UBQ3*: two independent lines; #1 and #2). Two-day-old etiolated seedlings were mock-, red light- (RL) or blue light- (BL) irradiated at 10 μmol m^{-2} s^{-1} for 6 h. Total proteins (10 μg) extracted from the seedlings were then separated on 10% SDS-PAGE gels, followed by immunoblotting with α-RPT2, α-PHOT2 and α-NPH3 antibodies. The protein-blotted membranes were stained as a loading control.

(C) Hypocotyl phototropism in wild-type (Col) seedlings and *35Spro:UBQ3* transgenic lines. Two-day-old etiolated seedlings were irradiated with unilateral blue light at 0.0017 or 0.17 μmol m^{-2} s^{-1} for 3 h, or 10 μmol m^{-2} s^{-1} for 6 h. The data shown are the mean values ± SE for hypocotyl curvatures of 14-24 seedlings. Asterisks indicate a statistically significant difference (Student's t test; $P < 0.05$).

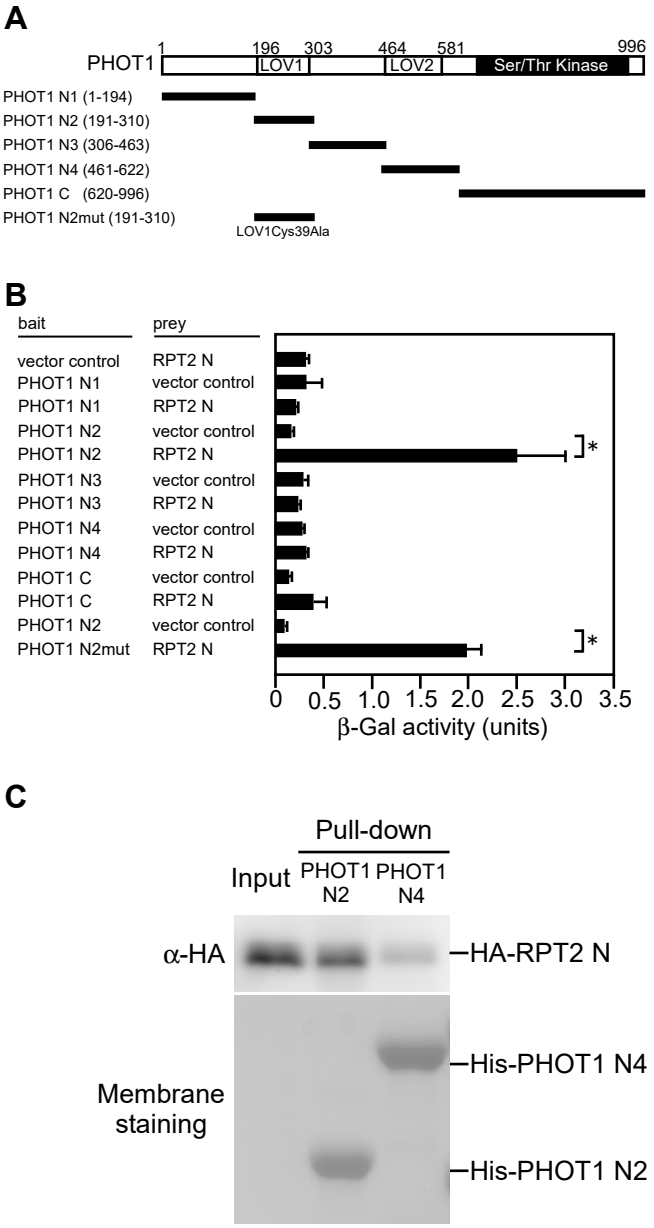

Figure 1. Interaction between phot1 and RPT2.
(A) Schematic representation of the phot1 structure. The Ser/The protein kinase and LOV domains are denoted by the solid and dotted blocks, respectively. The amino acid residues used for each underlined construct are indicated in parentheses.
(B) Yeast two-hybrid assay of phot1-RPT2 interactions. Solution assays of β-Gal activity were performed for the combinations indicated on the left. The data shown are means values ± SE (*n* = 3). The asterisk denotes statistically significant differences compared with the vector control (Student's t test; $P < 0.05$).
(C) In vitro pull-down assay to verify the interaction between the LOV domains of phot1 and the N-terminal half of RPT2. HA-tagged proteins of N-terminal half of the RPT2 (HA-RPT2 N) were incubated with the His-tagged LOV1 or LOV2 domains of phot1 for His-tag pull-down assay and detected by immunoblotting using anti-HA (α-HA) antibodies. The protein-blotted membrane were stained using a Pierce reversible protein staining kit.

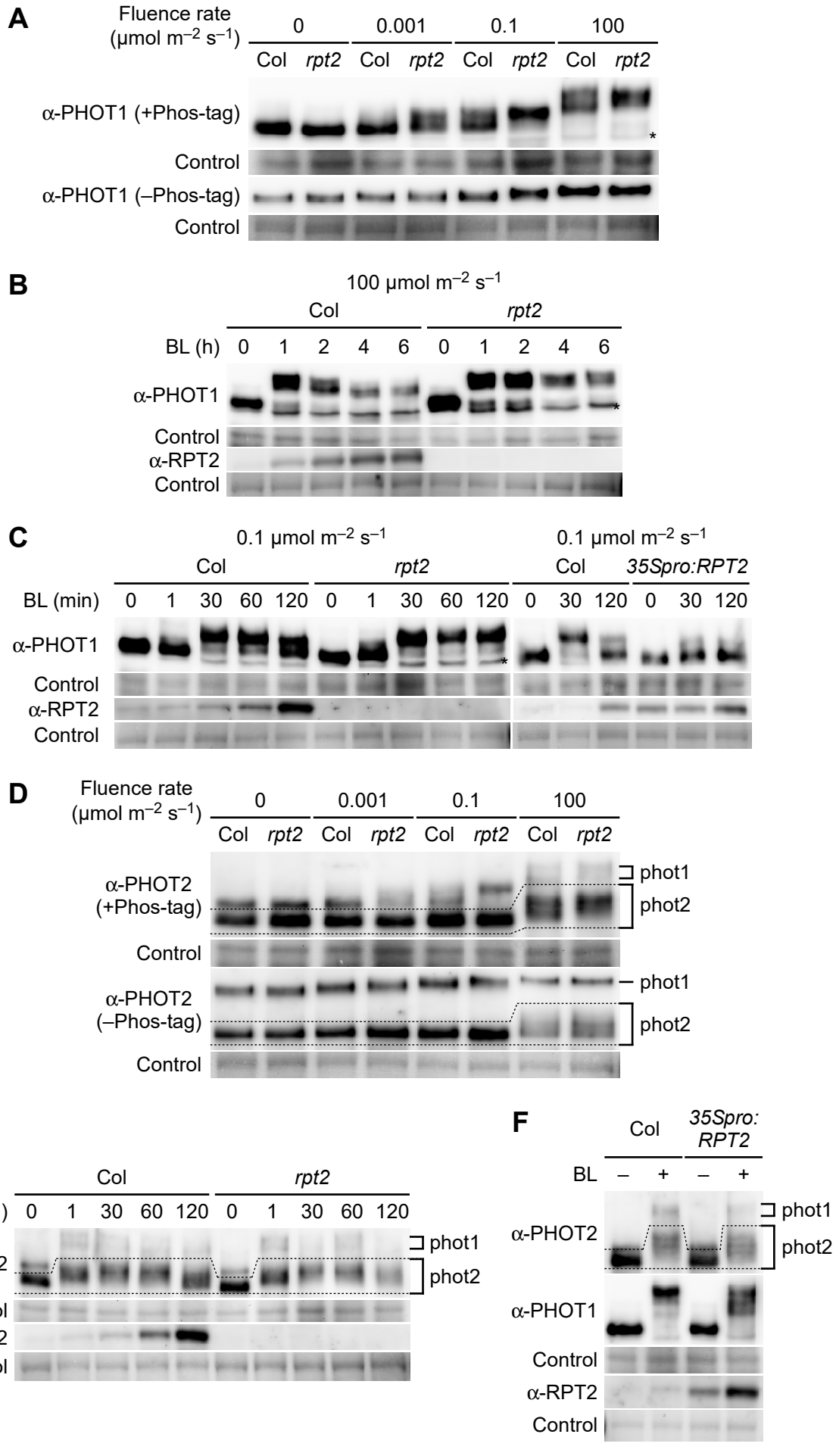

Figure 2. RPT2 suppresses the autophosphorylation of phot1.
(A) Immunoblotting analysis of PHOT1 in wild type (Col) and *rpt2* mutant *Arabidopsis*. Two-day-old etiolated seedlings were irradiated with unilateral blue light at the indicated fluence rates for 2 h. Total proteins (20 μg) extracted from the seedlings were separated on 6% SDS-PAGE gels with 2 μM Phos-tag (+ Phos-tag), followed by immunoblotting with anti-PHOT1 (α-PHOT1) antibodies. 10 μg of the total proteins were separated on 6% SDS-PAGE gels without Phos-tag (– Phos-tag) for comparison. An asterisk indicates a non-specific band. The protein-blotted membranes were stained as a loading control.
(B and C) Time course analysis of phot1 autophosphorylation. Two-day-old etiolated seedlings were irradiated with unilateral blue light at 100 μmol m^{-2} s^{-1} in **(B)** or 0.1 μmol m^{-2} s^{-1} in **(C)** for the indicated times. Other details are as described in **(A)**.
(D) Immunoblotting analysis of PHOT2 in wild type (Col) and *rpt2* mutant. Immunoblotting was performed with an anti-PHOT2 antibody (α-PHOT2) antibodies. Other details were as in **(A)**.
(E) Time course analysis of phot2 autophosphorylation. Two-day-old etiolated seedlings were irradiated with unilateral blue light at 100 μmol m^{-2} s^{-1} for the indicated times. Immunoblotting was performed with α-PHOT2 and anti-RPT2 (α-RPT2) antibodies. Other details are as described in **(A)**.
(F) Autophosphorylation of phot1 and phot2 in the *rpt2* mutant transformed with a *35Spro:RPT2* gene (*35Spro:RPT2*). Two-day-old etiolated seedlings were irradiated with unilateral blue light at 100 μmol m^{-2} s^{-1} for 30 minutes. Immunoblotting was performed with α-PHOT1, α-PHOT2 and α-RPT2 antibodies. Other details are as described in **(A)**.

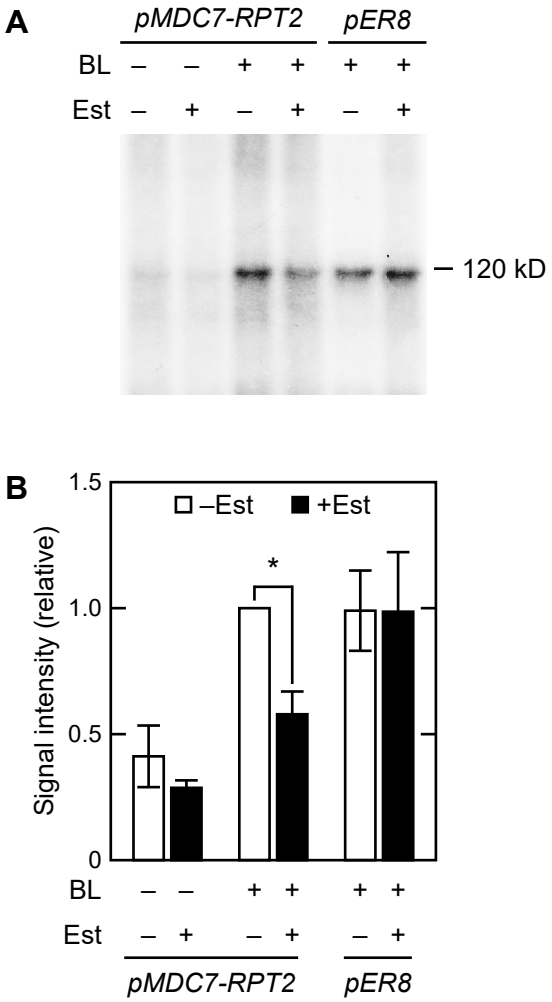

Figure 3. In vitro blue light-induced phosphorylation of a 120-kDa protein in microsomal membranes.

Two-day-old etiolated *rpt2* mutants transformed with a *pMDC7-RPT2* construct (*pMDC7-RPT2*) or wild-type seedlings transformed with a *pER8* vector control (*pER8*) were grown on agar medium with (–) or without (+) 10 μM estradiol (Est) under darkness. Microsomal proteins were then extracted.

(A) In vitro blue light-induced phosphorylation of a 120-kDa protein in microsomal membranes. Microsomal proteins were irradiated with mock (BL –) or blue light (BL +) at 10 μmol m^{-2} s^{-1} for 16 min in the presence of γ-^{32}P-ATP. The reacted samples were resolved on 6% SDS-PAGE gels and autoradiographed.

(B) Relative quantify of phosphorylated 120-kDa proteins. The value was calculated against the data from Est-untreated, blue light-irradiated *pMDC7-RPT2* seedlings. The data shown are mean values ± SE (n = 3). An asterisk indicate a statistically significant difference (Student's t test; $P < 0.05$).

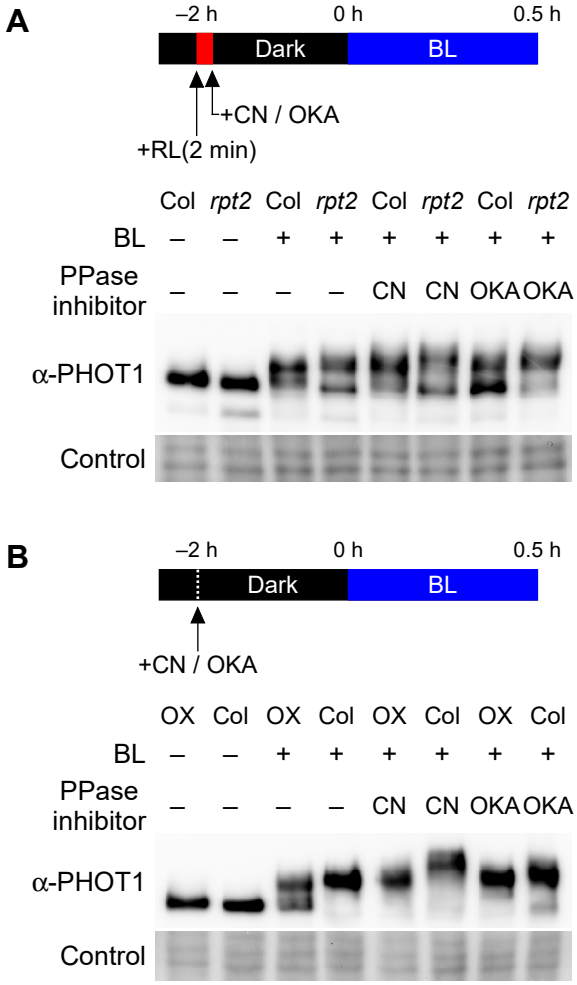

Figure 4. Effect of protein phosphatase inhibitors on phosphorylation status of phot1.
The aerial parts of two-day-old etiolated seedlings were incubated under darkness for 2 h in liquid medium with a protein phosphatase inhibitor (PPase inhibitor), 30 μM cantharidin (CN) or 1 μM okadaic acid (OKA), and subsequently treated with blue light at 0.1 μmol m^{-2} s^{-1} for 0.5 h. Total proteins (15 μg for **A**, 20 μg for **B**) extracted from the seedlings were separated on 6% SDS-PAGE gels with 2 μM Phos-tag, followed by immunoblotting with α-PHOT1 antibodies. Protein-blotted membranes were stained as a loading control.
(A) Effect of PPase inhibitors on the aerial parts of wild-type (Col) seedlings and *rpt2* mutants. Red light pretreatments were conducted to induce RPT2 expression before exposure to the PPase inhibitors.
(B) Effect of PPase inhibitors on the aerial parts of wild-type (Col) seedlings and the *35Spro:RPT2* lines (OX).

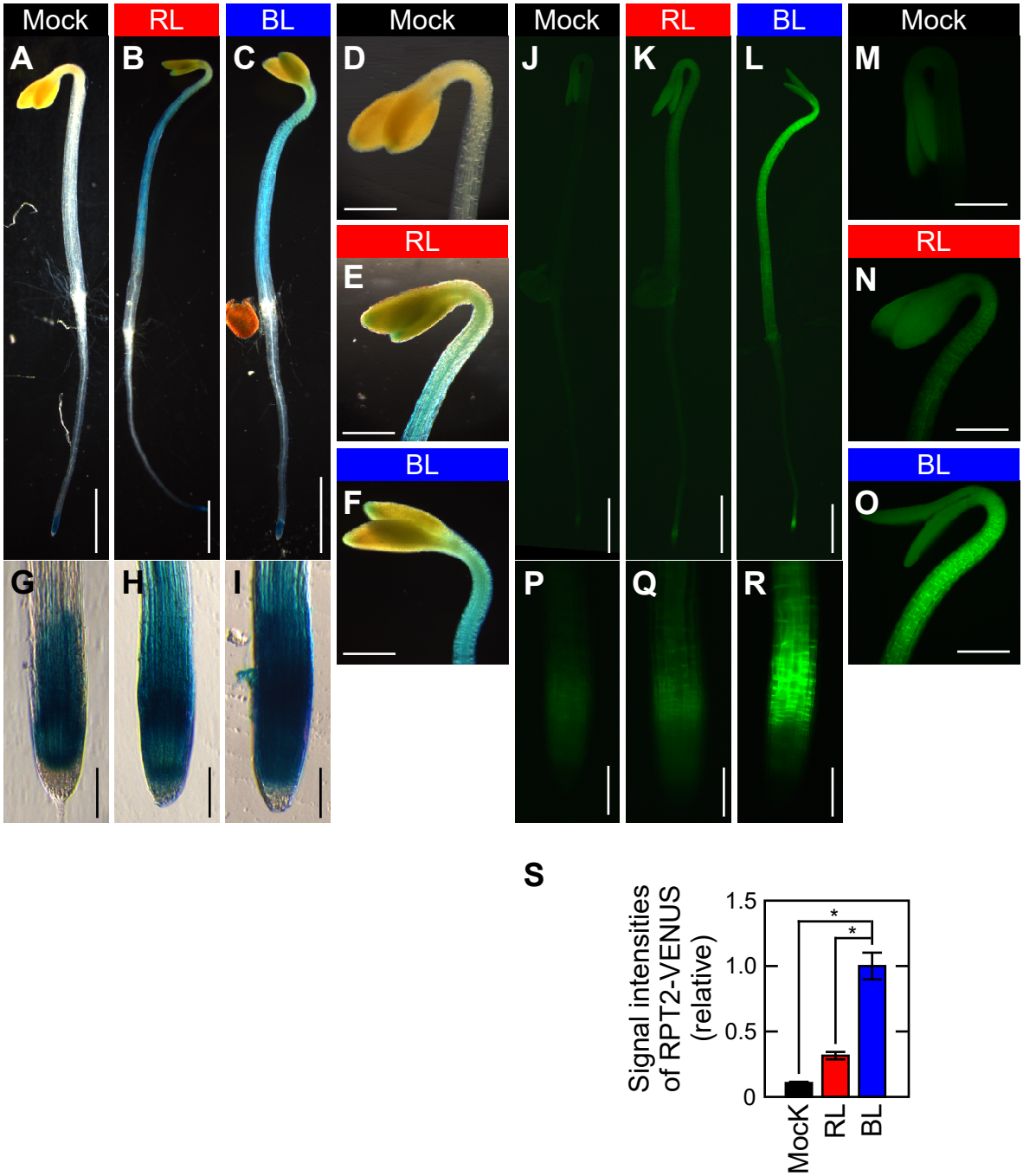

Figure 5. Expression patterns of the *RPT2pro:GUS* and the *RPT2pro:RPT2-VENUS* genes. Two-day-old etiolated seedlings were mock-irradiated **(**Mock: **A, D, G, J, M, P)**, or red light- **(**RL: **B, E, H, K, N, Q)** or blue light- **(**BL: **C, F, I, L, O, R)** irradiated at 10 μmol m^{-2} s^{-1} for 4 h. Scale bars: 1.0 mm **(A-C, J-I)**; 400 μm **(D-F, M-O)**; 100 μm **(G-I, P-R, U)**.
(A-I) GUS staining patterns of wild-type seedlings transformed with a *RPT2pro:GUS* gene.
(J-R) VENUS fluorescent images of the *rpt2* mutants transformed with a *RPT2pro:RPT2-VENUS* gene.
(S) Signal intensities of RPT2-VENUS fluorescence. Fluorescent signals were measured in the upper region of the hypocotyls and calculated relative to the value from BL-irradiated seedlings. The data shown are the mean values ± SE from 9 seedlings. Asterisks indicate a statistically significant difference (Student's t test; $P < 0.01$).

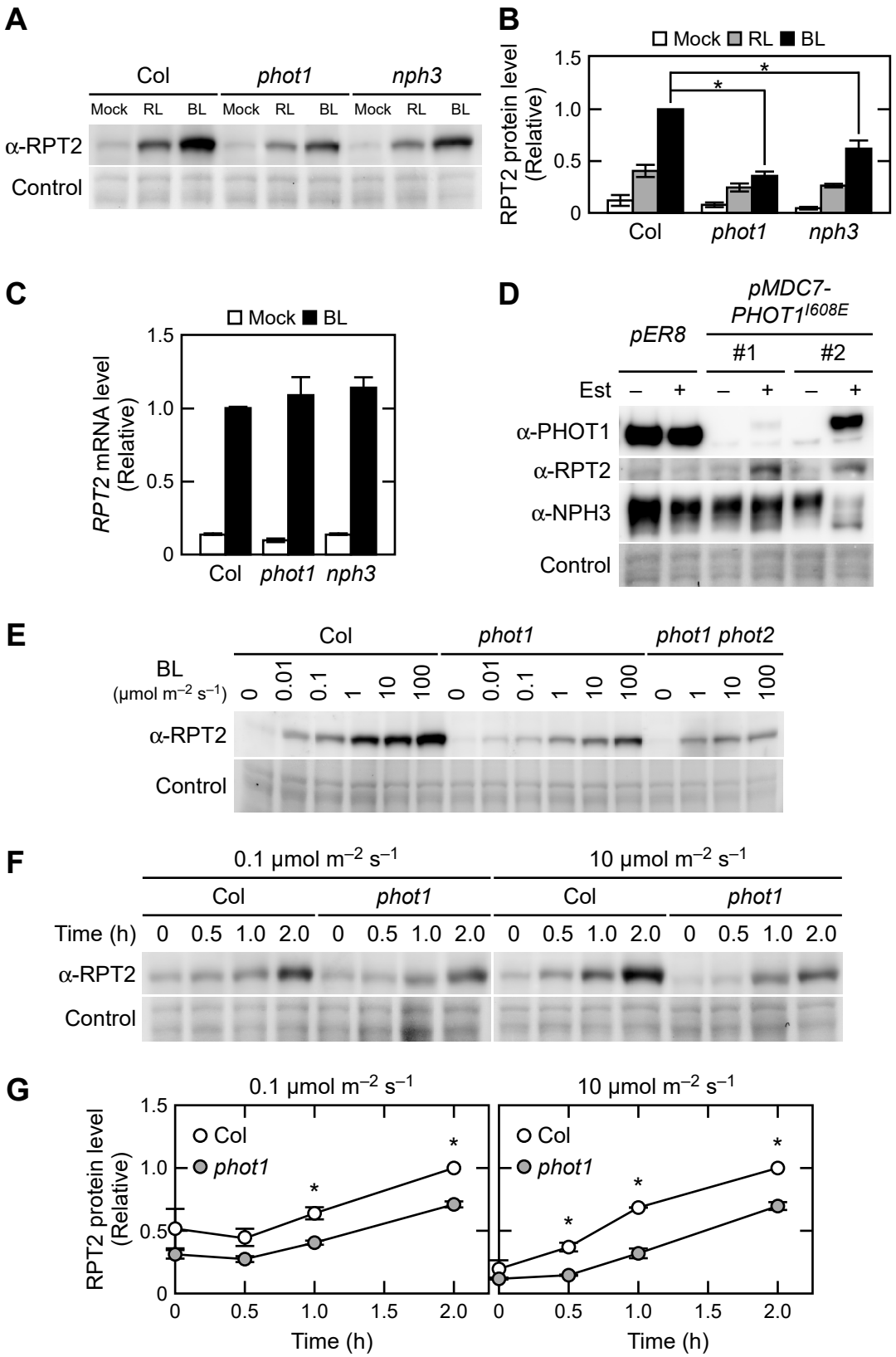

Figure 6. Post-transcriptinal regulation of RPT2 expression by phototropins.
(A) Immunoblotting analysis of RPT2 proteins in wild type (Col), *phot1*, and *nph3* seedlings. Two-day-old etiolated seedlings were mock-irradiated (Mock), or red light- (RL) or blue light- (BL) irradiated at 10 μmol m^{-2} s^{-1} for 6 h. Total proteins (10 μg) extracted from the seedlings were resolved on 10% SDS-PAGE gels, followed by immunoblotting with α-RPT2 antibodies. The protein-blotted membranes were stained as a loading control.
(B) Statistical analysis of the data in **(A)**. The values were normalized with a loading control and then calculated against the data from the blue light-irradiated seedlings of wild type. The data shown are the mean values ± SE (*n* = 3). Asterisks indicate a statistically significant difference (Student's t test; $P < 0.05$).
(C) qRT-PCR analysis of *RPT2* in wild type (Col), *phot1*, and *nph3* seedlings. Two-day-old etiolated seedlings were irradiated with blue light at 10 μmol m^{-2} s^{-1} for 6 h or mock-irradiated. The values were normalized using an internal control (*18S rRNA*) and the calculated against the values from blue light-irradiated seedlings of wild type. The data represent the means and SE (*n* = 3).
(D) Immunoblotting analysis of PHOT1, RPT2 and NPH3 in phot1 mutants transformed with a *pMDC7-PHOT1^{I608E}* construct (*pMDC7-PHOT1^{I608E}*: two independent lines, #1 and #2) and the *pER8* vector control line. Two-day-old etiolated seedlings were grown on agar medium with (+) or without (–) 10 μM estradiol (Est). Microsomal proteins (7.5 μg) extracted from the seedlings were separated on 7.5% SDS-PAGE gels, followed by immunoblotting with α-PHOT1, α-RPT2, and anti-NPH3 (α-NPH3) antibodies. The protein-blotted membranes were stained as a loading control.
(E) Fluence-rate dependency of the RPT2 induction in wild type (Col), *phot1*, and *phot1 phot2* double mutants. Two-day-old etiolated seedlings were irradiated with blue light at the indicated fluence rate for 6 h. Other details were as described in (**A**).
(F) Time course analysis of RPT2 induction in wild type (Col) and *phot1* seedlings. Two-day-old etiolated seedlings were irradiated with blue light at 0.1 (left panel) or 10 μmol m^{-2} s^{-1} (right panel) for the indicated period. Other details were as described in **(A)**.
(G) Statistical analysis the data generated in **(F)**. The values were normalized using a loading control and then calculated against the values from wild-type seedlings irradiated for 2 h. The data shown are the mean values ± SE (*n* = 3). Asterisks indicate a statistically significant difference (Student's t test; $P < 0.05$).

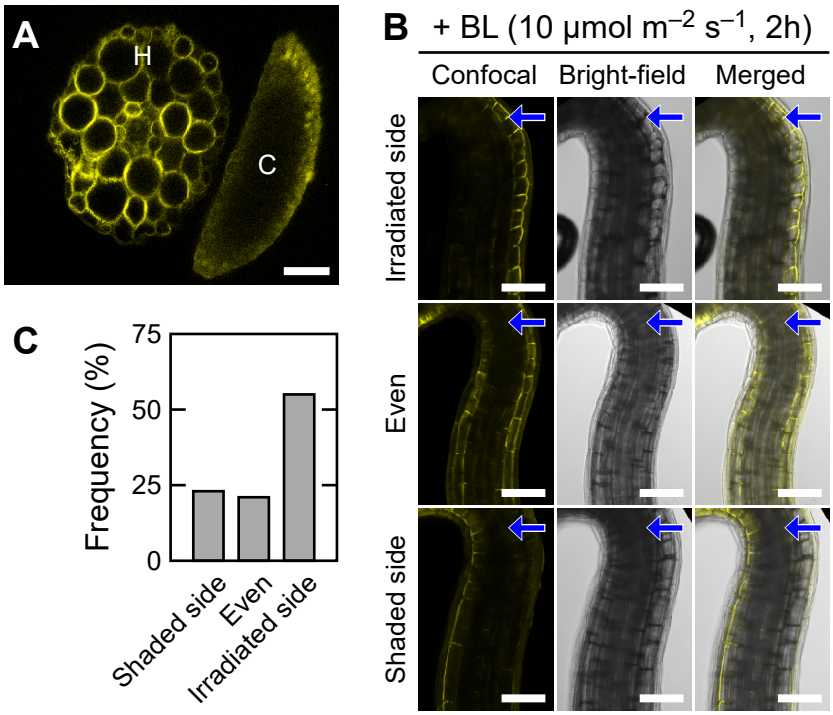

Figure 7. Distribution pattern of RPT2-VENUS protein in etiolated hypocotyls.
Two-day-old etiolated seedlings of *rpt2* mutants transformed with a *RPT2pro:RPT2-VENUS* gene were irradiated with blue light (BL) at 10 μmol m^{-2} s^{-1} for 6 h from above **(A)** or for 2 h from the unilateral side **(B)**.
(A) A typical distribution patten of RPT2-VENUS in the hypocotyl cross section. H, hypocotyl; C, cotyledon.
(B and C) Distribution patterns of RPT2-VENUS in the upper region of the hypocotyls. Distribution patterns were classified into three types (Irradiated side, Even and Shaded side). Representative confocal (left panel), bright field (mid panel) and merged images (right panel) are shown in **(B)**. Arrows indicate the direction of blue light. The frequencies of each expression pattern were calculated from 74 seedlings and are shown in **(C)**. White bar, 100 μm.

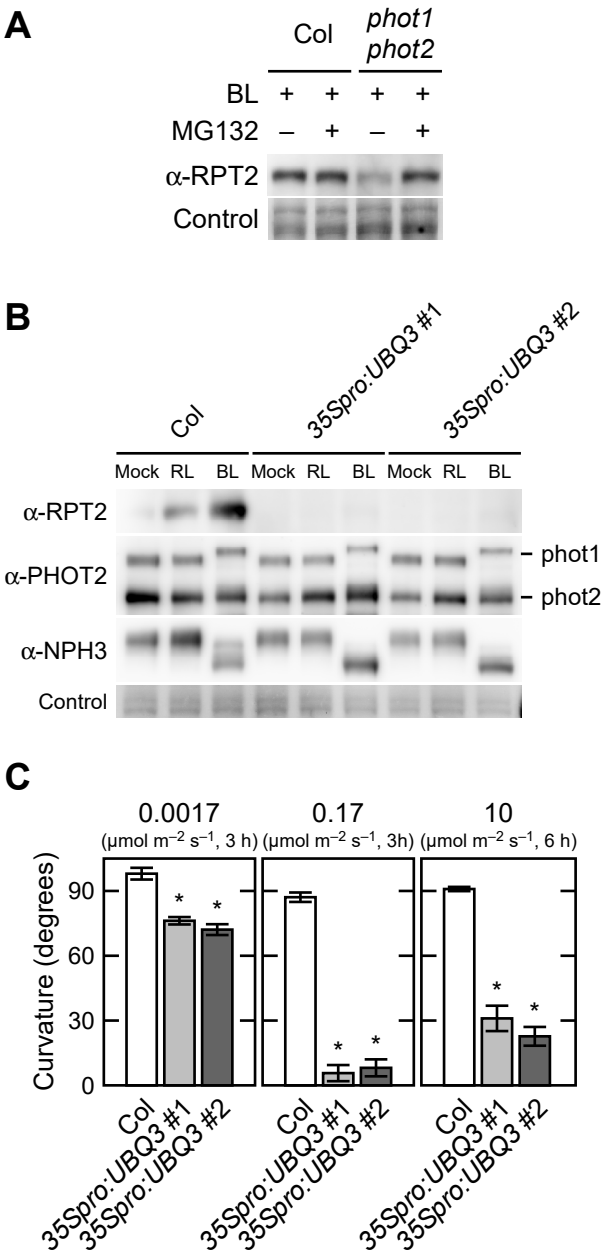

Figure 8. Destabilization of the RPT2 protein via a ubiquitin-proteasome dependent pathway.
(A) Effect of the proteasome inhibitor MG132 on RPT2 protein expression. Two-day-old etiolated seedlings of wild type (Col) and *phot1 phot2* double mutant were transferred into liquid medium with (+) or without (–) 50 μM MG132, kept in the dark for 1 h, and subsequently irradiated with blue light (BL) at 10 μmol m^{-2} s^{-1} for 3 h (+) or mock-irradiated (–). Total proteins (10 μg) extracted from the seedlings were separated on 10% SDS-PAGE gels, followed by immunoblotting with α-RPT2 antibodies. The protein-blotted membranes were stained as a loading control.
(B) Immunoblotting analysis of RPT2, PHOT1, PHOT2 and NPH3 in wild-type (Col) and wild-type seedlings transformed with *35Spro:UBQ3* (*35Spro:UBQ3*: two independent lines; #1 and #2). Two-day-old etiolated seedlings were mock-, red light- (RL) or blue light- (BL) irradiated at 10 μmol m^{-2} s^{-1} for 6 h. Total proteins (10 μg) extracted from the seedlings were then separated on 7.5% SDS-PAGE gels, followed by immunoblotting with α-RPT2, α-PHOT2 and α-NPH3 antibodies. The protein-blotted membranes were stained as a loading control.
(C) Hypocotyl phototropism in wild-type (Col) and *35Spro:UBQ3* transgenic lines. Two-day-old etiolated seedlings were irradiated with unilateral blue light at 0.0017 or 0.17 μmol m^{-2} s^{-1} for 3 h, or 10 μmol m^{-2} s^{-1} for 6 h. The data shown are the mean values ± SE for hypocotyl curvatures of 14-24 seedlings. Asterisks indicate a statistically significant difference (Student's t test; $P < 0.05$).

Parsed Citations

Alonso, J.M., Stepanova, A.N., Leisse, T.J., Kim, C.J., Chen, H., Shinn, P., Stevenson, D.K., Zimmerman, J., Barajas, P., Cheuk, R., Gadrinab, C., Heller, C., Jeske, A., Koesema, E., Meyers, C.C., Parker, H., Prednis, L., Ansari, Y., Choy, N., Deen, H., Geralt, M., Hazari, N., Hom, E., Karnes, M., Mulholland, C., Ndubaku, R., Schmidt, I., Guzman, P., Aguilar-Henonin, L., Schmid, M., Weigel, D., Carter, D.E., Marchand, T., Risseeuw, E., Brogden, D., Zeko, A., Crosby, W.L., Berry, C.C., and Ecker, J.R. (2003). Genome-Wide Insertional Mutagenesis of Arabidopsis thaliana. Science 301: 653-657.

Pubmed: Author and Title
Google Scholar: Author Only Title Only Author and Title

Ausubel, F.M., Brent, R., Kingston, R.E., Moore, D.D., Seidman, J.G., Smith, J.A., and Struhl, K. (2001). Current Protocols in Molecular Biology. New York, NY: John Wiley & Sons.

Pubmed: Author and Title
Google Scholar: Author Only Title Only Author and Title

Casal, J.J., Candia, A.N., and Sellaro, R. (2014). Light perception and signaling by phytochrome A. Journal of Experimental Botany 65: 2835-2845.

Pubmed: Author and Title
Google Scholar: Author Only Title Only Author and Title

Christie, J.M., Reymond, P., Powell, G.K., Bernasconi, P., Raibekas, A.A., Liscum, E., and Briggs, W.R. (1998). Arabidopsis NPH1: a flavoprotein with the properties of a photoreceptor for phototropism. Science 282: 1698-1701.

Pubmed: Author and Title
Google Scholar: Author Only Title Only Author and Title

Christie, J.M., Swartz, T.E., Bogomolni, R.A., and Briggs, W.R. (2002). Phototropin LOV domains exhibit distinct roles in regulating photoreceptor function. The Plant Journal 32: 205-219.

Pubmed: Author and Title
Google Scholar: Author Only Title Only Author and Title

Christie, J.M. (2007). Phototropin blue-light receptors. The Annual Review of Plant Biology 58: 21-45.

Pubmed: Author and Title
Google Scholar: Author Only Title Only Author and Title

Clough, R.C., and Vierstra, R.D. (1997). Phytochrome degradation. Plant, Cell & Environment 20: 713-721.

Pubmed: Author and Title
Google Scholar: Author Only Title Only Author and Title

Curtis, M.D., and Grossniklaus, U. (2003). A gateway cloning vector set for high-throughput functional analysis of genes in planta. Plant Physiol 133:462-469.

Pubmed: Author and Title
Google Scholar: Author Only Title Only Author and Title

de Wit, M., Galvão, V.C., and Fankhauser, C. (2016). Light-Mediated Hormonal Regulation of Plant Growth and Development. Annual Review of Plant Biology 67: 513-537.

Pubmed: Author and Title
Google Scholar: Author Only Title Only Author and Title

Genschik, P., Sumara, I., and Lechner, E. (2013). The emerging family of CULLIN3-RING ubiquitin ligases (CRL3s): cellular functions and disease implications. The EMBO Journal 32: 2307-2320.

Pubmed: Author and Title
Google Scholar: Author Only Title Only Author and Title

Haga, K., and Kimura, T. (2019). Physiological Characterization of Phototropism in Arabidopsis seedlings. In Method in Molecular Biology 1924 Phototropism, Yamamoto, K. T. ed (New York, USA: Human Press), pp. 3-17.

Pubmed: Author and Title
Google Scholar: Author Only Title Only Author and Title

Haga, K., and Sakai, T. (2012). PIN auxin efflux carriers are necessary for pulse-induced but not continuous light-induced phototropism in Arabidopsis. Plant Physiol. 160: 763-776.

Pubmed: Author and Title
Google Scholar: Author Only Title Only Author and Title

Haga, K., Tsuchida-Mayama, T., Yamada, M., and Sakai, T. (2015). Arabidopsis ROOT PHOTOTROPISM2 Contributes to the Adaptation to High-Intensity Light in Phototropic Responses. The Plant Cell. 27: 1098-1112.

Pubmed: Author and Title
Google Scholar: Author Only Title Only Author and Title

Harada, A., Takemiya, A., Inoue, S., Sakai, T., and Shimazaki, K. (2013). Role of RPT2 in leaf positioning and flattening and a possible inhibition of phot2 signaling by phot1. Plant & Cell Physiology 54: 36-47.

Pubmed: Author and Title
Google Scholar: Author Only Title Only Author and Title

Harper, S.M., Christie, J.M., and Gardner, K.H. (2004). Disruption of the LOV-J□ helix interaction activates phototropin kinase activity.

Biochemistry 43: 16184-16192.
Pubmed: Author and Title
Google Scholar: Author Only Title Only Author and Title

Inada, S., Ohgishi, M., Mayama, T., Okada, K., and Sakai, T. (2004). RPT2 is a signal transducer involved in phototropic response and stomatal opening by association with phototropin 1 in Arabidopsis thaliana. The Plant Cell 16: 886-897.
Pubmed: Author and Title
Google Scholar: Author Only Title Only Author and Title

Kagawa, T., Sakai, T., Suetsugu, N., Oikawa, K., Ishiguro, S., Kato, T., Tabata, S., Okada, K., and Wada, M. (2001). Arabidopsis NPL1: a phototropin homolog controlling the chloroplast high-light avoidance response. Science 291: 2138-2141.
Pubmed: Author and Title
Google Scholar: Author Only Title Only Author and Title

Kaiserli, E., Sullivan, S., Jones, M.A., Feeney, K.A., and Christie, J.M. (2009). Domain swapping to assess the mechanistic basis of Arabidopsis phototropin 1 receptor kinase activation and endocytosis by blue-light. Plant Cell. 21: 3226-3244.
Pubmed: Author and Title
Google Scholar: Author Only Title Only Author and Title

Kinoshita, T., Doi, M., Suetsugu, N., Kagawa, T., Wada, M., and Shimazaki, K. (2001). Phot1 and phot2 mediate blue light regulation of stomatal opening. Nature 414: 656-660.
Pubmed: Author and Title
Google Scholar: Author Only Title Only Author and Title

Kinoshita, E., and Kinoshita-Kikuta, E. (2011). Improved Phos-tag SDS-PAGE under neutral pH conditions for advanced protein phosphorylation profiling. Proteomics 11: 319-323.
Pubmed: Author and Title
Google Scholar: Author Only Title Only Author and Title

Li, J., Li, G., Wang, H., and Deng, X.Q. (2011). Phytochrome signaling mechanism. The Arabidopsis Book e0148.
Pubmed: Author and Title
Google Scholar: Author Only Title Only Author and Title

Lin, C., Yang, H., Guo, H., Mockler, T., Chen, J., and Cashmore, A.R. (1998). Enhancement of blue-light sensitivity of Arabidopsis seedlings by a blue light receptor cryptochrome 2. Proceedings of the National Academy of Sciences of the United States of America 95: 2686-2690.
Pubmed: Author and Title
Google Scholar: Author Only Title Only Author and Title

Liscum, E., and Briggs, W.R. (1995). Mutations in the NPH1 locus of Arabidopsis disrupt the perception of phototropic stimuli. The Plant Cell 7: 473-485.
Pubmed: Author and Title
Google Scholar: Author Only Title Only Author and Title

Motchoulski, A., and Liscum, E. (1999). Arabidopsis NPH3: A NPH1 photoreceptor-interacting protein essential for phototropism. Science 286: 961-964.
Pubmed: Author and Title
Google Scholar: Author Only Title Only Author and Title

Nagashima, A., Suzuki, G., Uehara, Y., Saji, K., Furukawa, T., Koshiba, T., Sekimoto, M., Fujioka, S., Kuroha, T., Kojima, M., Sakakibara, H., Fujisawa, N., Okada, K., and Sakai, T. (2008). Phytochromes and cryptochromes regulate the differential growth of Arabidopsis hypocotyls in both a PGP19-dependent and -independent manner. The Plant Journal 53, 516-529.
Pubmed: Author and Title
Google Scholar: Author Only Title Only Author and Title

Nakasako, M., Iwata, T., Matsuoka, D., and Tokutomi, S. (2004). Light-induced structural changes of LOV domain-containing polypeptides from Arabidopsis phototropin 1 and 2 studied by small-angle X-ray scattering. Biochemistry 43: 14881-14890.
Pubmed: Author and Title
Google Scholar: Author Only Title Only Author and Title

Ohgishi, M., Saji, K., Okada, K., and Sakai, T. (2004). Functional analysis of each blue-light receptor, cry1, cry2, phot1, and phot2, by using combinatorial multiple mutants in Arabidopsis. Proceedings of the National Academy of Sciences of the United States of America 101: 2223-2228.
Pubmed: Author and Title
Google Scholar: Author Only Title Only Author and Title

Okajima, K., Kashojiya, S., and Tokutomi, S. (2012). Photosensitivity of kinase activation by blue-light involves the lifetime of a cysteinyl-flavin adduct intermediate, S390, in the photoreaction cycle of the LOV2 domain in phototropin, a plant blue-light receptor. Journal of Biological Chemistry 287: 40972-40981.
Pubmed: Author and Title
Google Scholar: Author Only Title Only Author and Title

Okajima, K. (2016). Molecular mechanism of phototropin light signaling. Journal of Plant Research 129: 159-166.
Pubmed: Author and Title
Google Scholar: Author Only Title Only Author and Title

Pedmale, U.V., and Liscum, E. (2007). Regulation of phototropic signaling in Arabidopsis via phosphorylation state changes in the phototropin 1-interacting protein NPH3. Journal of Biological Chemistry 282: 19992-20001.
Pubmed: Author and Title
Google Scholar: Author Only Title Only Author and Title

Petersen, J., Inoue, S.I., Kelly, S.M., Sullivan, S., Kinoshita, T., and Christie, J.M. (2017). Functional characterization of a constitutively active kinase variant of Arabidopsis phototropin 1. Journal of Biological Chemistry 292: 13843-13852.
Pubmed: Author and Title
Google Scholar: Author Only Title Only Author and Title

Rademacher, E.H., and Offringa, R. (2012). Evolutionary Adaptations of Plant AGC Kinases: From Light Signaling to Cell Polarity Regulation. Frontiers in Plant Science 3: 250.
Pubmed: Author and Title
Google Scholar: Author Only Title Only Author and Title

Roberts, D., Pedmale, U.V., Morrow, J., Sachdev, S., Lechner, E., Tang, X., Zheng, N., Hannink, M., Genschik, P., and Liscum, E. (2011). Modulation of phototropic responsiveness in Arabidopsis through ubiquitination of phototropin 1 by the CUL3-Ring E3 ubiquitin ligase CRL3 (NPH3). The Plant Cell 23: 3627-3640.
Pubmed: Author and Title
Google Scholar: Author Only Title Only Author and Title

Sakai, T., Wada, T., Ishiguro, S., and Okada, K. (2000). RPT2. A signal transducer of the phototropic response in Arabidopsis. The Plant Cell 12: 225-236.
Pubmed: Author and Title
Google Scholar: Author Only Title Only Author and Title

Sakai, T., Kagawa, T., Kasahara, M., Swartz, T.E., Christie, J.M., Briggs, W.R., Wada, M., and Okada, K. (2001). Arabidopsis nph1 and npl1: blue-light receptors that mediate both phototropism and chloroplast relocation. Proceedings of the National Academy of Science of America 98: 6969-6974.
Pubmed: Author and Title
Google Scholar: Author Only Title Only Author and Title

Sakai, T. (2005). NPH3 and RPT2: signal transducers in phototropin signaling pathways. In Light Sensing in Plants, Wada M, Shimazaki K, Iino M eds (Tokyo, Japan: Springer-Verlag), pp. 179-184.
Pubmed: Author and Title
Google Scholar: Author Only Title Only Author and Title

Sakamoto, K., and Briggs, W.R. (2002). Cellular and subcellular localization of phototropin 1. The Plant Cell 14: 1723-1735.
Pubmed: Author and Title
Google Scholar: Author Only Title Only Author and Title

Schindelin, J., Arganda-Carreras, I., Frise, E., Kaynig, V., Longair, M., Pietzsch, T., Preibisch, S., Rueden, C., Saalfeld, S., Schmid, B., et al. (2012) Fiji: An open-source platform for biological-image analysis. Nat Methods 9: 676–68
Pubmed: Author and Title
Google Scholar: Author Only Title Only Author and Title

Sharrock, R.A., and Clack, T. (2002). Patterns of expression and normalized levels of the five Arabidopsis phytochromes. Plant Physiology 130: 442-456.
Pubmed: Author and Title
Google Scholar: Author Only Title Only Author and Title

Sullivan, S., Thomson, C.E., Lamont, D.J., Jones, M.A., and Christie, J.M. (2008). In vivo phosphorylation site mapping and functional characterization of Arabidopsis phototropin 1. Molecular Plant 1: 178-194.
Pubmed: Author and Title
Google Scholar: Author Only Title Only Author and Title

Sullivan, S., Kharshiing, E., Laird, J., Sakai, T., and Christie, J.M. (2019). Deetiolation Enhances Phototropism by Modulating NON-PHOTOTROPIC HYPOCOTYL3 Phosphorylation Status. Plant Physiology 180: 1119-1131.
Pubmed: Author and Title
Google Scholar: Author Only Title Only Author and Title

Suetsugu, N., Takemiya, A., Kong, S.G., Higa, T., Komatsu, A., Shimazaki, K., Kohchi, T., and Wada, M. (2016). RPT2/NCH1 subfamily of NPH3-like proteins is essential for the chloroplast accumulation response in land plants. Proceedings of the National Academy of Science of America 113: 10424-10429.
Pubmed: Author and Title
Google Scholar: Author Only Title Only Author and Title

Suzuki, H., Koshiba, T., Fujita, C., Yamauchi, Y., Kimura, T., Isobe, T., Sakai, T., Taoka, M, and Okamoto, T. (2019). Low-fluence blue light-induced phosphorylation of Zmphot1 mediates the first positive phototropism. Journal of Experimental Botany in press.
Pubmed: Author and Title
Google Scholar: Author Only Title Only Author and Title

Tsuchida-Mayama, T., Nakano, M., Uehara, Y., Sano, M., Fujisawa, N., Okada, K., and Sakai, T. (2008). Mapping of the phosphorylation

sites on the phototropic signal transducer, NPH3. Plant Science 174: 626-633.
Pubmed: Author and Title
Google Scholar: Author Only Title Only Author and Title

Tsuchida-Mayama, T., Sakai, T., Hanada, A., Uehara, Y., Asami, T., and Yamaguchi, S. (2010). Role of the phytochrome and cryptochrome signaling pathways in hypocotyl phototropism. The Plant Journal 62: 653-662.
Pubmed: Author and Title
Google Scholar: Author Only Title Only Author and Title

Xue, Y., Xing, J., Wan, Y., Lv, X., Fan, L., Zhang, Y., Song, K., Wang, L., Wang, X., Deng, X., Baluška, F., Christie, J.M., and Lin, J. (2018). Arabidopsis Blue-light Receptor Phototropin 1 Undergoes Blue-light-Induced Activation in Membrane Microdomains. Molecular Plant 11: 846-859.
Pubmed: Author and Title
Google Scholar: Author Only Title Only Author and Title

Zuo, J., Niu, Q.W., and Chua, N.H. (2000). An estrogen receptor-based transactivator XVE mediates highly inducible gene expression in transgenic plants. The Plant Journal 24: 265-273.
Pubmed: Author and Title
Google Scholar: Author Only Title Only Author and Title